Biogeosciences, 9, 3405–3423, 2012
www.biogeosciences.net/9/3405/2012/
doi:10.5194/bg-9-3405-2012

Biogeosciences

Organic matter exudation by *Emiliania huxleyi* under simulated future ocean conditions

C. Borchard[1,2] **and A. Engel**[2]

[1]Alfred Wegener Institute for Polar and Marine Research, Bremerhaven, Germany
[2]GEOMAR – Helmholtz Centre for Ocean Research, Kiel, Germany

Correspondence to: A. Engel (aengel@geomar.de)

Received: 15 December 2011 – Published in Biogeosciences Discuss.: 27 January 2012
Revised: 20 July 2012 – Accepted: 31 July 2012 – Published: 27 August 2012

Abstract. *Emiliania huxleyi* (strain B 92/11) was exposed to different nutrient supply, CO_2 and temperature conditions in phosphorus controlled chemostats to investigate effects on organic carbon exudation and partitioning between the pools of particulate organic carbon (POC) and dissolved organic carbon (DOC). ^{14}C incubation measurements for primary production (PP) and extracellular release (ER) were performed. Chemical analysis included the amount and composition of high molecular weight (>1 kDa) dissolved combined carbohydrates (HMW-dCCHO), particulate combined carbohydrates (pCCHO) and the carbon content of transparent exopolymer particles (TEP-C). Applied CO_2 and temperature conditions were 300, 550 and 900 µatm pCO_2 at 14 °C, and additionally 900 µatm pCO_2 at 18 °C simulating a greenhouse ocean scenario.

Enhanced nutrient stress by reducing the dilution rate (D) from $D = 0.3\,d^{-1}$ to $D = 0.1\,d^{-1}$ ($D = \mu$) induced the strongest response in *E. huxleyi*. At $\mu = 0.3\,d^{-1}$, PP was significantly higher at elevated CO_2 and temperature and $DO^{14}C$ production correlated to $PO^{14}C$ production in all treatments, resulting in similar percentages of extracellular release (PER; ($DO^{14}C$ production/PP) × 100) averaging 3.74 ± 0.94 %. At $\mu = 0.1\,d^{-1}$, $PO^{14}C$ production decreased significantly, while exudation of $DO^{14}C$ increased. Thus, indicating a stronger partitioning from the particulate to the dissolved pool. Maximum PER of 16.3 ± 2.3 % were observed at $\mu = 0.1\,d^{-1}$ at elevated CO_2 and temperature.

While cell densities remained constant within each treatment and throughout the experiment, concentrations of HMW-dCCHO, pCCHO and TEP were generally higher under enhanced nutrient stress. At $\mu = 0.3\,d^{-1}$, pCCHO concentration increased significantly with elevated CO_2 and temperature. At $\mu = 0.1\,d^{-1}$, the contribution (mol % C) of HMW-dCCHO to DOC was lower at elevated CO_2 and temperature while pCCHO and TEP concentrations were higher. This was most pronounced under greenhouse conditions. Our findings suggest a stronger transformation of primary produced DOC into POC by coagulation of exudates under nutrient limitation. Our results further imply that elevated CO_2 and temperature will increase exudation by *E. huxleyi* and may affect organic carbon partitioning in the ocean due to an enhanced transfer of HMW-dCCHO to TEP by aggregation processes.

1 Introduction

Primary production (PP) in the sunlit surface ocean is the driving force for the uptake of CO_2 and basis for its potential sequestration into the ocean's interior (Chisholm, 2000; Falkowski et al., 2000). The production of particulate organic carbon (POC) via PP is accompanied by the extracellular release (ER) of various amounts of dissolved organic carbon (DOC). ER represents a significant fraction of PP (Myklestad, 1977; Mague et al., 1980; Baines and Pace, 1991) and was reported from a variety of phytoplankton species in several studies over the last decades (Fogg, 1966; Myklestad, 1995; Biddanda and Benner, 1997; Descy et al., 2002; Wetz and Wheeler, 2007; López-Sandoval et al., 2011). Results from a modelling study with data from coastal, marine and estuarine systems revealed a linear relationship between PP and ER for non-freshwater systems with a percentage of extracellular release (PER) in a range of 2–50 % (Baines and Pace, 1991). A correlation between PP and ER was shown for irradiance (constant daylength) and temperature for marine

(Verity et al., 1991) and freshwater algae (Zlotnik and Dubinsky, 1989) as long as applied conditions are in a range of optimum conditions of the tested algae. Data obtained under nutrient limitation frequently revealed PP and ER to be decoupled, generally leading to significantly higher PER (Myklestad, 1977; Obernosterer and Herndl, 1995; López-Sandoval et al., 2011). PER for marine phytoplankton typically ranges between 2–10 % (Nagata, 2000) or between 20–40 % in oligotrophic regions (Karl et al., 1998; Teira et al., 2001; López-Sandoval et al., 2011). This suggests that a fraction of photosynthesates (e.g., organic carbon) is not used for the build-up of biomass during nutrient limitation, but is discharged from the cell. Exudation of excess photosynthesates was suggested to be more energy-efficient for the phytoplankton cell than intracellular storage (Wangersky, 1978; Wood and van Valen, 1990). Maintaining the photosynthetic activity while bearing a loss of organic carbon may be additionally interpreted as a strategy to effectively shorten the lag phase for resuming the full photosynthetic capacity when nutrients become available again (Fogg, 1983).

Changes in the partitioning of POC and DOC have strong implications for carbon export fluxes, because DOC itself, unlike POC, does not sink. DOC can only be transported to deeper waters by mixing processes, e.g., downwelling and eddy diffusion (Kaehler et al., 1997; Ducklow et al., 2001; Karl et al., 2001). However, if not subject to bacterial degradation, freshly produced DOC accumulates in surface waters and may affect the transfer efficiency of dissolved compounds into the particulate size spectrum of POC (>0.7 µm) via coagulation processes: Exudates provide precursors for transparent exopolymer particles (TEP) (Passow, 2000), which represent an abiotic linkage between DOC and POC in marine carbon cycling (Chin et al., 1998; Wells, 1998; Engel et al., 2004b; Verdugo et al., 2004; Verdugo et al., 2008; Gogou and Repeta, 2010). Phytoplankton exudates are by up to 80 % comprised by carbohydrates (Myklestad, 1977, 1995; Ittekkot et al., 1981; Lancelot, 1984; Myklestad et al., 1989) which are, therefore, expected to play an important role for the TEP formation (Engel, 2004b).

Since preindustrial times, emissions of the greenhouse gas CO_2 into the atmosphere increased due to human activities (Caldeira and Wickett, 2003; Meehl et al., 2007). According to future projections on climate change, a rise in CO_2 and temperature will occur simultaneously (IPCC, Solomon et al., 2007) most likely accompanied by a reduced nutrient availability in the photic zone due to enhanced stratification of the ocean's surface (Boyd and Doney, 2002; Sarmiento et al., 2004). The sea surface is expected to be most affected by global change (Raven et al., 2005) and acidification and warming will likely influence the photosynthetic fixation of CO_2 and, therefore, the ocean's organic carbon pump and the fate of organic matter in the ocean (Falkowski, 1994; Arrigo, 2007; Caldeira, 2007).

Particulate and dissolved organic carbon production and therefore carbon fluxes were hypothesised to be affected by CO_2 and temperature (Engel, 2002; Leonardos and Geider, 2005; Moran et al., 2006; Wohlers et al., 2009; Kim et al., 2011). In accordance, TEP concentration has been shown to be related to seawater CO_2-concentrations (Engel, 2002; Moran et al., 2006) and its formation was reported to be enhanced at elevated temperature (Claquin et al., 2008). Several studies report on enhanced exudation of TEP-precursors at nutrient stress (Staats et al., 2000; Passow, 2002a; Underwood et al., 2004), as a consequence of carbon overflow (Schartau et al., 2007). Factors that influence carbon overconsumption, exudation and TEP-formation will, thus, affect elemental ratios of particulate organic matter (POM) and may have strong implications for the organic carbon pump (Engel, 2002; Schneider et al., 2004). However, ER in referred studies was deduced from DOC accumulation rather than from direct rate measurements.

Emiliania huxleyi, a cosmopolitan species of coccolithophores, was the subject of several studies in the context of global change (Riebesell et al., 2000; Zondervan et al., 2002; Sciandra et al., 2003; Delille et al., 2005; Leonardos and Geider, 2005; Feng et al., 2008; Langer et al., 2009). Phytoplankton blooms dominated by *Emiliania huxleyi* were regularly observed at high irradiances in stratified waters where nitrate is abundant, but phosphate concentrations are well below 0.3 µmol l^{-1} (Veldhuis et al., 1994; Van der Wal et al., 1995; Head et al., 1998), in regions such as the North Sea to the east of the Shetland Islands or the Bjørnafjorden, Norway. *E. huxleyi* was frequently shown to grow well on low phosphate concentrations (Egge and Heimdal, 1994; Paasche, 2002) and was, therefore, suggested to be a strong competitor in phosphate depleted regions or situations in the ocean (Riegman et al., 2000).

E. huxleyi primary production was shown to be stimulated by elevated partial pressure of CO_2 (pCO_2) (Riebesell et al., 2000, 2007; Egge et al., 2009) and elevated temperature (Langer et al., 2007; Feng et al., 2008). Studies with *E. huxleyi* reporting on effects of nutrient limitation in the context of global change are scarce, but a clear decoupling of nutrient assimilation from carbon assimilation at high CO_2 conditions has been shown for nitrate (Sciandra et al., 2003) and phosphate limitation (Leonardos and Geider, 2005; Borchard et al., 2011). ER of organic carbon and the production of extracellular polysaccharides was reported for *E. huxleyi* previously (Nanninga et al., 1996; Biddanda and Benner, 1997; Godoi et al., 2009). Furthermore, the presence of coccolith polysaccharides (CP) (Westbroek et al., 1973), as well as the carbohydrate composition of CP in this species is well described (De Jong et al., 1979; Fichtinger Schepman et al., 1979; Kayano and Shiraiwa, 2009). Galacturonic acid, an acidic polysaccharide, was determined in *E. huxleyi* cultures (Nanninga et al., 1996) and is of great interest, since polysaccharides in general and acidic polysaccharides in particular, are known to facilitate TEP-formation (Mopper et al., 1995; Passow, 2000, 2002b).

Results on the elemental composition of *E. huxleyi* in response to phosphorus limitation, CO_2 and temperature conditions during a chemostat experiment were presented in Borchard et al. (2011). High C : P ratios of particulate matter were observed during that study and were most pronounced at elevated CO_2 and combined high CO_2 and temperature. Elevated CO_2 also sustained higher biomass (e.g., cell densities) on identical nutrient supply. This led to a remarkable low P quota in high CO_2 cells potentially representing a minimum quota for sustaining growth at the given rate.

Here, we give detailed information on dissolved and particulate primary production derived from the same experiment in order to assess information on the partitioning of DOC and POC derived from *E. huxleyi* as a function of nutrient availability, CO_2 and temperature. The main objectives during the present study were to determine (i) the partitioning of photosynthetically produced POC and DOC, (ii) the amount and composition of high molecular weight (>1 kDa) dissolved combined carbohydrates (HMW-dCCHO) and particulate CCHO (pCCHO) and (iii) to test for linkages to TEP-formation.

2 Methods

2.1 Experimental setup

Data shown here were obtained during the chemostat experiment described in more detail by Borchard et al. (2011). Briefly, a calcifying strain of *Emiliania huxleyi* (PML B92/11) was grown in CO_2- and temperature-controlled chemostats with a culture volume of 9.2 l. Nutrient medium for the constant supply was prepared from sterile-filtered (Sartobran P, 0.2 µm capsule, Sartorius) natural seawater (SW) with a salinity of 32, pH of 7.97 and total alkalinity (TA) of 2281 µmol kg^{-1} SW. SW was enriched with nutrients to yield final concentrations of 29 µmol l^{-1} NO_3^- and 1.1 µmol l^{-1} PO_4^{3-} and with a metal mix according to the f/2-recipe (Guillard and Ryther, 1962). Medium for each chemostat was stored in 100 l reservoirs. In order to sterilize the medium, it was treated with UV irradiation (Microfloat 1/0, a.c.k. aqua concept GmbH) for 3 h before the addition of sterile-filtered f/2-vitamins (0.2 µm, Minisart, Sartorius).

After filling 9.2 l nutrient medium into each chemostat incubator, CO_2 and temperature conditions of 300 and 550 µatm at 14 °C and 900 µatm at 14 and 18 °C were applied and treatments are hereafter referred to as 300-14, 550-14, 900-14 and 900-18. CO_2-concentrations in chemostats were achieved by constant aeration with gas obtained from a CO_2 regulation system based on the mixing of CO_2 free air and pure CO_2 using mass flow controllers (MFC, Type 1179 Mass Flo Controller; MKS Instruments, Germany) (Borchard et al., 2011). Briefly, premixed gases were channelled into each incubator via silicon and gas distribution tubes (ROBU; Type A, Por. 1) and allowed to equilibrate for 2 d before inoculation with cells. Each chemostat incubator was surrounded by a water jacket connected to a thermostat (Lauda, Ecoline Staredition, RE 104) setting temperatures to target values ±0.1 °C. A 16 h:8 h light:dark cycle with a photon flux density of 300 µmol photons m^{-2} s^{-1} was applied (TL-D Delux Pro, Philips; QSL 100, Biospherical Instruments, Inc.).

All pipes and tubes connected to the incubator were rinsed first with 10 % hydrochloric acid (HCl), subsequently with deionised water and then sterilized by autoclaving at 121 °C for 30 min before usage. The incubator and the reservoir vessels were cleaned with phosphate-free detergent, then soaked in 10 % HCl for 2 h and thoroughly rinsed with deionised water thereafter.

After the 2 days of CO_2 equilibration (considered as the first and second day of the experiment), cells were inoculated to each chemostat to a density of 3000 cells ml^{-1} and grown in batch mode for 3 d until the constant medium supply was applied for 12 d at a dilution rate (D) of $D = 0.3\ d^{-1}$ followed by 12 d at $D = 0.1\ d^{-1}$.

Aeration with gas of preset CO_2 concentrations was maintained throughout the experiment in incubators and medium reservoirs. Gentle mixing at 50 rotations min^{-1} by a mechanical stirrer inside the incubator kept cells in suspension. Three samplings were accomplished during steady state of each growth rate at 8 a.m. (three hours after lights went on) and are referred to hereafter as sampling 1, 2 and 3 for $\mu = 0.3\ d^{-1}$ (10, 14 and 17 days after the start of the experiment) and sampling 4, 5 and 6, for $\mu = 0.1\ d^{-1}$ (22, 25 and 28 days after the start of the experiment).

2.2 Analytical methods

$PO^{14}C$ production (µmol l^{-1} d^{-1}) was measured using the ^{14}C incubation method according to Steemann Nielsen (1952) and Gargas (1975). 50 ml samples were taken in triplicates from each chemostat, transferred into cell culture flasks (25 cm^2, Corning) and spiked with approximately 5 µCi $NaHCO_3^-$ (Hartmann Analytics, specific activity 40–60 mCi/mmole). Each triplicate set was incubated for 4 h at the same light and temperature conditions of the original chemostat treatment, but without aeration. Simultaneously, dark uptake was determined in triplicate for each treatment from 50 ml sample wrapped in aluminium foil and incubated in the dark for 4 h. Activity in the samples was determined by removing a 100 µl aliquot from three dark bottles prior to incubation and transferred to 6 ml liquid scintillation vials in which 200 µl of 2N NaOH were placed. 4 ml of liquid scintillation cocktail were added thereafter. All incubations were stopped by gentle filtration on 0.4 µm polycarbonate filters (Nuclepore) at <150 mbar to avoid cell breakage. After rinsing with 10 ml sterile filtered seawater, filters were treated with fuming HCl in order to remove inorganic ^{14}C. Filters were transferred to 6 ml scintillation vials, 4 ml liquid scintillation cocktail (Ultima Gold AB) were added and samples

were stored overnight before being counted in a Packard Tri Carb Liquid Scintillation Counter. Carbon incorporation rates were calculated in accordance to Gargas (1975) by implementing the values of total dissolved organic carbon determined on the respective sampling day for each chemostat.

Exuded dissolved organic carbon ($DO^{14}C$ production; $\mu mol\,l^{-1}\,d^{-1}$) was measured in the 0.4 µm-filtrate obtained during the $PO^{14}C$-filtration. 4 ml liquid sample were acidified with 100 µl 2 M HCl and left for 7 days in a desiccator with a NaOH-trap at ∼600 mbar depression to allow for outgassing of inorganic ^{14}C. After the addition of 15 ml liquid scintillation cocktail (Ultima Gold AB), overnight storage, counting and calculations were accomplished as described above.

Primary Production (PP; µmol C $l^{-1}\,d^{-1}$) was derived from the sum of the production of $PO^{14}C$ and $DO^{14}C$ ($PO^{14}C$ production + $DO^{14}C$ production = PP). The percentage of extracellular release (PER) was calculated as ($DO^{14}C$ production/PP) × 100).

Concentrations of PP, $PO^{14}C$ and $DO^{14}C$ (x [µmol l^{-1}]) were derived from production rates (γ [µmol $l^{-1}\,d^{-1}$]) by applying the following equation with μ being the growth rate [d^{-1}]:

$$x\,[\mu mol\,l^{-1}] = \frac{\gamma\,[\mu mol\,l^{-1}\,d^{-1}]}{\mu[d^{-1}]} \quad (1)$$

Cell normalised concentrations of PP, $PO^{14}C$ and $DO^{14}C$ (x_{cell} [pmol $cell^{-1}$]) were derived from cell normalised production rates (γ_{cell} [pmol $cell^{-1}\,d^{-1}$]) by applying the following equation:

$$x_{cell}\,[pmol\,cell^{-1}] = \frac{\gamma_{cell}\,[pmol\,cell^{-1}\,d^{-1}]}{\mu[d^{-1}]} \quad (2)$$

The analysis of high molecular weight (HMW, >1 kDa) dissolved combined carbohydrates (HMW-dCCHO) and of total combined carbohydrates >1 kDa (tCCHO), were conducted by ion chromatographie. Duplicate samples for HMW-dCCHO were filtered through 0.45 µm syringe-filters (GHP membrane, Acrodisk, Pall Corporation) and stored in precombusted (8 h at 500 °C) glass vials at −20 °C. Samples for tCCHO remained unfiltered and were stored identically. Prior to analysis, samples were desalinated by membrane dialysis (1 kDa MWCO, Spectra Por) for 6 h at 0 °C. Thereafter, samples were hydrolysed with HCl at a final concentration of 0.8 M for 20 h at 100 °C to yield monomeric CHO. Samples were stored at −20 °C overnight and then neutralised by acid evaporation (N_2) at 50 °C. Dried samples were solubilised in ultra-pure water before determination of CHO monomers by high performance anion exchange chromatography (HPAEC) coupled with pulsed amperometric detection (PAD) on a Dionex ICS 3000 following Engel and Händel (2011). Separation of combined fucose (Fuc), rhamnose (Rha), arabinose (Ara)/galactosamine (GalN) (quantified together due to coelution), glucosamine (GlcN), galactose (Gal), glucose (Glc), mannose (Man)/xylose (Xyl) (quantified together due to coelution), galacturonic acid (Gal-URA) and glucuronic acid (Glc-URA) was achieved by applying a Dionex CarboPac PA10 guard column (2 × 50 mm) coupled to a Dionex CarboPac PA10 analytical column (2 × 250 mm). Detection limits were 10 nM. Particulate CCHO (pCCHO) were determined by substracting HMW-dCCHO from tCCHO. Concentrations of CCHO are given as mol carbon per liter (mol C l^{-1}).

Transparent exopolymer particles (TEP) were determined according to the colorimetric method by Passow and Alldredge (1995). 10 to 20 ml sample were filtered in triplicate onto 0.4 µm polycarbonate filters (Nuclepore), stained with Alcian Blue and rinsed with several ml of ultrapure water. Filters were stored in polypropylene tubes at −20 °C until analysis. TEP-concentrations are given in units of µg Xanthan-equivalents per litre (µg $X_{eq.}\,l^{-1}$). Conversation to carbon-units (TEP-C) in µmol C l^{-1} was done by applying a factor of $f_0 = 0.63$ as suggested by Engel et al. (2004a). Alcian Blue was shown to stain the surface of *E. huxleyi* coccoliths. Therefore, TEP-C concentrations were corrected for the amount of Alcian Blue per cell as described by Engel et al. (2004a).

Cell densities were determined daily as the mean of three consecutive measurements of 500 µl sample with a Beckman Coulter Counter (Coulter Multisizer III) equipped with a 100 µm aperture. Prior to measurements, samples were diluted 1:100 with 0.2 µm pre-filtered (Minisart, Sartorius) seawater with a salinity of 32. The equivalent spherical diameter (ESD) of *E. huxleyi* was determined to be within a particle size range of 3.27–7.96 µm, based on microscopic measurements. A constant cell density over three consecutive days (maximum variation of 10 %) was accepted as criterion for steady state growth in continuous cultures after Leonardos and Geider (2005).

During the present study, bacterial cell numbers were checked by flow cytometry and numbers were low and similar in all treatments. We estimated the carbon demand from growth rate and an assumed biomass of 20 fg C bacterial $cell^{-1}$ (Lee and Fuhrman, 1987), a growth efficiency of 30 % and assuming that 70 % of carbon uptake was respired. Relative to the huge concentrations of organic carbon produced by *E. huxleyi*, the bacterial carbon demand was negligible for the present study.

For nutrients, 50 ml sample were filtered through 0.2 µm (Minisart 2000, Sartorius) syringe filters and frozen at −20 °C until analysis. NO_3^- and PO_4^{3-} were determined spectrophotometrically after Grasshoff et al. (1999) (Autoanalyser Evolution 3, Alliance Instruments). Detection limits were 0.3 µmol l^{-1} for N and 0.1 µmol l^{-1} for P.

For particulate organic carbon (POC), nitrogen (PON) and phosphorus (POP), 100 ml sample were filtered in duplicates onto pre-combusted (8 h at 500 °C) glass fibre filters (GF/F, Whatman). POC filters were acidified by adding 3–5 drops of 0.2 M HCl on top of the filter to remove particulate inorganic

Table 1. Total alkalinity (TA), partial pressure of CO_2 (pCO_2), cell densities and cell quota for particulate organic carbon (POC), nitrogen (PON) and phosphorus (POP). Mean values and standard deviations (in parentheses, for TA and pCO_2 as %) were derived from sampling 1, 2 and 3 ($\mu = 0.3\,d^{-1}$) and from sampling 4, 5 and 6 ($\mu = 0.1\,d^{-1}$), respectively.

μ [d^{-1}]	Treatment	TA (µmol kg^{-1} SW)	pCO_2 (µatm)	Cell density [$\times 10^5\,l^{-1}$]	POC [pmol $cell^{-1}$]	PON [pmol $cell^{-1}$]	POP [fmol $cell^{-1}$]
0.3	300-14	1440 (1.9 %)	243 (9.7 %)	2940 (166)	1.84 (0.13)	0.072 (0.001)	2.86 (0.01)
	550-14	1435 (1.1 %)	522 (1.7 %)	3294 (187)	1.81 (0.06)	0.069 (0.003)	2.70 (0.29)
	900-14	1517 (0.5 %)	924 (12.5 %)	3574 (274)	1.68 (0.07)	0.070 (0.002)	2.41 (0.13)
	900-18	1309 (1.8 %)	902 (13.6 %)	4243 (125)	1.77 (0.00)	0.060 (0.000)	2.47 (0.48)
0.1	300-14	1031 (1.9 %)	274 (12.3 %)	3177 (184)	2.69 (0.21)	0.066 (0.006)	3.09 (0.21)
	550-14	1095 (4.6 %)	546 (1.3 %)	2941 (247)	2.70 (0.13)	0.070 (0.007)	2.84 (0.23)
	900-14	1260 (1.6 %)	1056 (0.5 %)	3663 (368)	2.52 (0.32)	0.070 (0.007)	2.50 (0.30)
	900-18	1153 (1.7 %)	994 (0.8 %)	4168 (324)	2.46 (0.12)	0.061 (0.002)	2.19 (0.08)

carbon and dried overnight at 60 °C. C- and N-concentrations were determined with an elemental analyser (EuroEA, Euro Vector). Total nitrogen (TN) concentrations were calculated as the sum of residual concentrations of inorganic N in the chemostats and PON.

For dissolved organic phosphorous (DOP), 35 ml GF/F filtrate were stored frozen at −20 °C until analysis. POP and DOP were determined colorimetrically after persulfate oxidation with a precision of $\pm 0.02\,\mu mol\,l^{-1}$ (Koroleff and Grasshof, 1983). Total phosphorus (TP) concentrations were calculated from residual concentrations of inorganic P in the chemostats (below the detection limit during steady state of the present experiment and, therefore, $0\,\mu mol\,l^{-1}$) and DOP + POP.

The carbonate chemistry during the experiment is described in more detail in Borchard et al. (2011) and was determined from pH and total alkalinity (TA). Briefly, pH values in the treatments were measured with a proton sensitive combined pH-temperature electrode (Sentix 41; WTW standard DIN/NBS buffers PL 4, PL 7 and PL 9) and recorded hourly on a data logger (WTW; pH 340i) throughout the experiment. For TA, 200 ml of sample were filtered through combusted (8 h, 500 °C) glass fibre filters (GF/F, Whatman) and analysed by the titration method with 0.1 M HCl (Gran, 1952). pCO_2, total dissolved inorganic carbon (DIC), carbonate (CO_3^{2-}), bicarbonate (HCO_3^-) and Ω calcite in each treatment and medium reservoirs were calculated from $pH_{(NBS)}$ and TA values at the beginning of the experiment and at each sampling day using the programme CO2sys (Lewis and Wallace, 1998). After equilibration with distinct CO_2-gas concentrations, initial pH values ranged from 8.29 to 7.86 at a TA value of 2281 µmol kg^{-1} seawater, representing a CO_2 range from 287 ± 6 and 897 ± 17 µatm CO_2. Carbonate chemistry was strongly affected by biological activity of *E. huxleyi*, but remained constant within each dilution rate (Table 1). The complete dataset for the carbonate chemistry and related discussion is given elsewhere (Borchard et al., 2011, in Sect. 4.3 and Tables 1 and 3).

2.3 Data treatment

During steady state growth, the total production rates (γ [µmol l^{-1} d^{-1}]) for CCHO and TEP-C were calculated from concentrations (x [µmol l^{-1}]) and growth rates (μ [d^{-1}]) by applying the following equation:

$$\gamma\,[\mu mol\,l^{-1}\,d^{-1}] = x\,[\mu mol\,l^{-1}] \times \mu[d^{-1}] \quad (3)$$

Cell normalised production rates (γ_{cell}; fmol $cell^{-1}$ d^{-1}) were derived from cell normalised concentrations of CCHO and TEP-C (x_{cell}; fmol $cell^{-1}$) with n being the cell density by the use of the following equation:

$$\gamma_{cell}\,[fmol\,cell^{-1}\,d^{-1}] = \frac{x\,[\mu mol\,L^{-1}]}{n\,[l^{-1}]} \times \mu[d^{-1}] \quad (4)$$

Mean values ± standard deviations for each dilution rate were derived from sampling 1, 2 and 3 ($\mu = 0.3\,d^{-1}$) and 4, 5 and 6 ($\mu = 0.1\,d^{-1}$), respectively. Contributions (mol %) and elemental ratios are consistently derived from concentrations (mol l^{-1}: mol l^{-1}). Differences between treatments were tested by means of analysis of variance (two-way ANOVA), and by means of t-tests. Statistical treatment of data was performed by using the software package SigmaPlot 10.01 (SysStat).

3 Results

3.1 Nutrients and cell densities

Supply media of all chemostats was enriched to identical nutrient concentrations of $29\,\mu mol\,l^{-1}$ NO_3^- and $1.1\,\mu mol\,l^{-1}$ PO_4^{3-}. Data on cell densities and elemental stoichiometry in the course of the experiment are given in more detail in Borchard et al. (2011). Briefly, growth of *E. huxleyi* was stimulated by a rise in CO_2 and temperature during the initial nutrient replete batch phase and during the transition to phosphorus limitation. While cell densities within each treatment

remained constant throughout the experiment after reaching the steady state (5 to 7 days after setting the dilution rate (D) to $D = 0.3\,d^{-1}$), cell densities differed significantly (t-test, $n = 17$, $p < 0.001$) between treatments ranging from $3138 \times 10^5 \pm 8.1\,\%$ cells l^{-1} in the 300-14 treatment and maximum $4238 \times 10^5 \pm 7.5\,\%$ cells l^{-1} in the 900-18 treatment (Table 1). Cell densities remained stable throughout both dilution rates with a maximum variation of 10.2 % (550-14), indicating that growth rates balanced dilution rates with $\mu = D = 0.3\,d^{-1}$ and $\mu = D = 0.1\,d^{-1}$.

PO_4^{3-} and dissolved organic phosphorus concentrations were below the detection limit in all treatments for both growth rates. Residual DIN concentrations of 0.42–1.08 µmol l^{-1} were determined in culture media of all treatments, indicating exclusive phosphorus depletion. Average PON:POP ratios were 25.5 ± 3.0 and similar for all treatments. Cell quota for POP (P quota) exhibited a decreasing trend with increasing CO_2 and temperature reflecting the differences in cell densities produced on identical nutrient concentrations (Table 1). A minimum P quota of 2.19±0.08 fmol $cell^{-1}$was determined for cells growing at $D = 0.1\,d^{-1}$ (900-18).

3.2 Primary production

Primary production (PP) was strongly affected by differences in nutrient supply, CO_2 and temperature conditions (Fig. 1, upper panel). PP was significantly higher at $\mu = 0.3\,d^{-1}$ than at $\mu = 0.1\,d^{-1}$ (two way ANOVA, $p < 0.001$). At $\mu = 0.3\,d^{-1}$, PP increased significantly with CO_2 and temperature (two way ANOVA, Holm-Sidak-Method, $p < 0.005$) from 153.6 ± 8.6 µmol C $l^{-1}\,d^{-1}$ (300-14) to 230.3 ± 12.9 µmol C $l^{-1}\,d^{-1}$ (900-18). At $\mu = 0.1\,d^{-1}$, PP ranged between 106.3 ± 33.4 µmol C $l^{-1}\,d^{-1}$ (300-14) and 96.9 ± 4.9 µmol C $l^{-1}\,d^{-1}$ (900-14) and did not differ between treatments (Fig. 1, upper panel).

Nutrient, CO_2 and temperature conditions also affected the partitioning of primary produced organic carbon into $DO^{14}C$ and $PO^{14}C$. At $\mu = 0.3\,d^{-1}$, $DO^{14}C$ production ranged between 6.02 ± 2.57 µmol C $l^{-1}\,d^{-1}$ (550-14) and 8.59 ± 2.85 µmol C $l^{-1}\,d^{-1}$ (900-18) and correlated with $PO^{14}C$ production in all treatments (Fig. 1, middle panel). This led to an average percentage of extracellular release (PER) of $3.74 \pm 0.94\,\%$ at $\mu = 0.3\,d^{-1}$ (Fig. 1, lower panel). Relative to $\mu = 0.3\,d^{-1}$, $PO^{14}C$ production at $\mu = 0.1\,d^{-1}$ was up to 61 % (900-18) lower (two way ANOVA, $p \leq 0.013$). $DO^{14}C$ production increased in all treatments at $\mu = 0.1\,d^{-1}$, ranging between 9.38 ± 3.29 µmol C $l^{-1}\,d^{-1}$ (550-14) and 17.06 ± 1.71 µmol C $l^{-1}\,d^{-1}$ (900-18) (Fig. 1, middle panel). This opposite effect of nutrient limitation on $PO^{14}C$ and $DO^{14}C$ production yielded an average PER of $11.00 \pm 4.64\,\%$ at $\mu = 0.1\,d^{-1}$, significantly higher than at $\mu = 0.3\,d^{-1}$ (two way ANOVA, $p < 0.001$). At $\mu = 0.1\,d^{-1}$, highest values for PER of $16.29 \pm 2.33\,\%$ were observed for 900-18, significantly different from the other treatments (two way ANOVA, Holm-Sidak-Method, $p = 0.004$) (Fig. 1, lower panel).

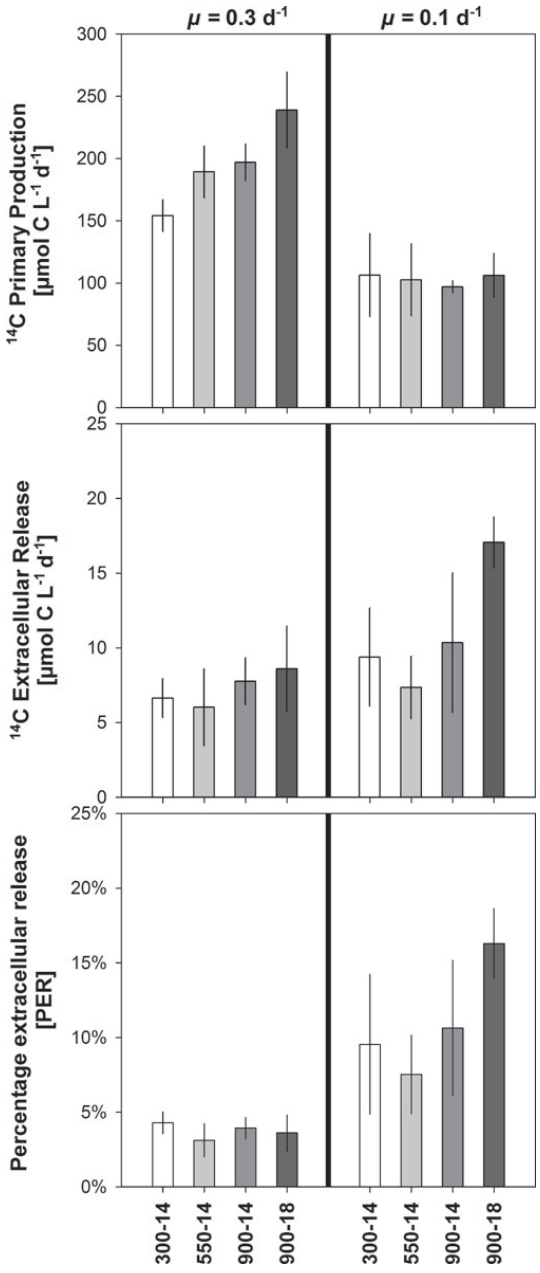

Fig. 1. Primary Production (upper panel), extracellular release (middle panel) and percentage of extracellular release (PER, lower panel) at various growth-, CO_2 and temperature conditions. Mean values and standard deviations were derived from sampling 1, 2 and 3 ($\mu = 0.3\,d^{-1}$) and sampling 4, 5 and 6 ($\mu = 0.1\,d^{-1}$), respectively.

Averaging for all treatments, $DO^{14}C$:total nitrogen (TN) ratios increased significantly from 1.0 ± 0.1 at $\mu = 0.3\,d^{-1}$, to a range of 3.7 ± 0.9 (550-14) to 7.2 ± 0.9 (900-18) at $\mu = 0.1\,d^{-1}$ ($p < 0.001$). A stronger decoupling of exudation and nutrient assimilation as a result of enhanced phosphorus

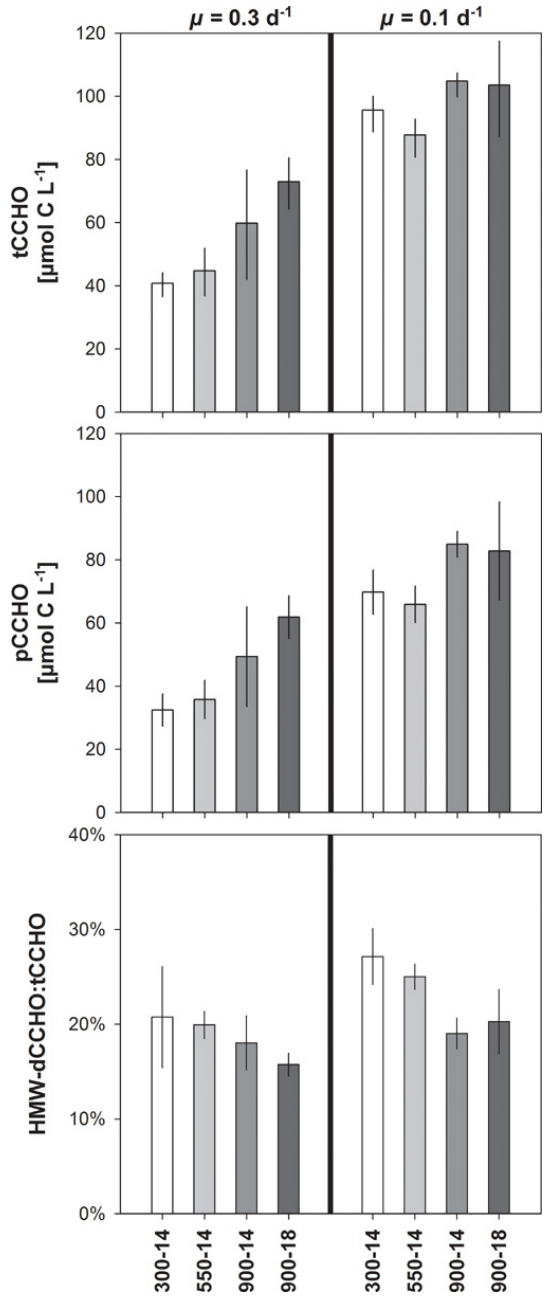

Fig. 2. Total combined carbohydrates (tCCHO, upper panel), particulate CCHO (pCCHO, middle panel) and contribution (mol % C) of high molecular weight (>1 kDa) dissolved CCHO (HMW-dCCHO) to tCCHO (lower panel) at various growth-, CO_2 and temperature conditions. Mean values and standard deviations were derived from sampling 1, 2 and 3 ($\mu = 0.3\,d^{-1}$) and sampling 4, 5 and 6 ($\mu = 0.1\,d^{-1}$), respectively.

limitation was visible in $DO^{14}C$:total phosphorus (TP) ratios. At $\mu = 0.3\,d^{-1}$, ratios varied between 20.7 ± 3.2 (500-14) to 29.0 ± 8.3 (900-18) and increased clearly to a range between 91.8 ± 30.7 (550-14) and 199.4 ± 24.7 (900-18) at $\mu = 0.1\,d^{-1}$.

3.3 Particulate and dissolved combined carbohydrates

Combined carbohydrate (CCHO) concentration varied significantly due to changed nutrient, CO_2 and temperature conditions (Two way ANOVA, Holm-Sidak-Method, $p < 0.001$) (Fig. 2, upper panel).

At $\mu = 0.3\,d^{-1}$, tCCHO were affected by CO_2 and temperature conditions and were significantly higher at 900-18 than at 300-14 and 550-14 (two way ANOVA, Holm-Sidak-Method, $p = 0.001$ and $p = 0.002$). Concentrations of tCCHO ranged between 40.7 ± 3.8 (300-14) and 73.0 ± 8.3 µmol C l^{-1} (900-18) (Fig. 2, upper panel). The CO_2 and temperature induced increase in tCCHO concentration was primarily due to pCCHO which showed a similar trend as tCCHO in a range of 32.4 ± 5.1 (300-14) and 61.8 ± 6.8 µmol C l^{-1} (900-18) (Fig. 2, middle panel). Accordingly, pCCHO in both high CO_2 treatments (900-14 and 900-18) were significantly higher than pCCHO derived from 300-14 and 550-14 (Two way ANOVA, Holm-Sidak-Method, $p \leq 0.009$).

Concentrations of pCCHO and HMW-dCCHO in all treatments were significantly higher at $\mu = 0.1\,d^{-1}$ compared to $\mu = 0.3\,d^{-1}$ (two way ANOVA, $p < 0.001$). Reducing the nutrient supply yielded the strongest relative increase in pCCHO concentration at 300-14. However, highest absolute concentrations of pCCHO at $\mu = 0.1\,d^{-1}$ were still observed at 900-14 and 900-18 (Table 2 and Fig. 2, middle panel). This was also reflected in tCCHO concentrations which increased with CO_2 from 87.8 ± 6.1 (550-14) to 104.8 ± 3.7 µmol C l^{-1} (900-14) (Fig. 2, upper panel).

The higher concentrations of pCCHO at $\mu = 0.1\,d^{-1}$ compared to $\mu = 0.3\,d^{-1}$ were most pronounced for Man/Xyl ($p < 0.001$), Fuc ($p < 0.001$), Rha ($p \leq 0.004$, except for 900-18 in which Rha decreased), Ara/GalN ($p < 0.001$), GlcN ($p \leq 0.001$), Gal ($p \leq 0.026$, except for 900-18), Glc ($p \leq 0.001$), and Gal-URA ($p \leq 0.001$). Concentrations of Glc-URA were unaffected by the change of growth rate (Table 3).

HMW-dCCHO at $\mu = 0.3\,d^{-1}$ ranged between 8.3 ± 1.4 (300-14) and 11.5 ± 1.4 µmol C l^{-1} (900-18) and concentrations increased with increasing CO_2 and temperature (Table 2). HMW-dCCHO concentrations were significantly higher at $\mu = 0.1\,d^{-1}$ than at $\mu = 0.3\,d^{-1}$ (two way ANOVA, $p < 0.001$) and ranged between 25.8 ± 1.4 (300-14) and 19.9 ± 1.5 µmol l^{-1} (900-14). The increase of HMW-dCCHO was primarily induced by significantly higher concentrations of dissolved Fuc ($p < 0.001$), Rha ($p \leq 0.004$), Ara/GalN ($p < 0.001$), GlcN ($p \leq 0.021$, except for 900-18), Gal ($p \leq 0.001$), Glc ($p \leq 0.016$, except for 900-14 and 900-18), Man/Xyl ($p < 0.001$) and Gal-URA ($p \leq 0.032$). Concentrations of Glc-URA were unaffected by the change of growth rate (Table 3).

Averaged for all treatments, HMW-dCCHO comprised 18.6 ± 3.4 % of tCCHO with lowest proportions of 15.8 ± 1.2 % in 900-18 (Fig. 2, lower panel). Partitioning between HMW-dCCHO and pCCHO at $\mu = 0.3\,d^{-1}$ was clearly

Table 2. Total concentrations (µmol C l^{-1}) and cell normalised production (fmol C $cell^{-1}$ d^{-1}) of particulate combined carbohydrates (pCCHO) and high molecular weight (>1 kDa) dissolved CCHO (HMW-dCCHO), particulate ($PO^{14}C$) and dissolved ($DO^{14}C$) organic carbon at various CO_2, temperature and growth conditions. Cell normalised concentrations for TEP-C (fmol C $cell^{-1}$), and contributions (mol % C) of pCCHO to $PO^{14}C$ and HMW-dCCHO to $DO^{14}C$ are given. Concentrations (µmol l^{-1}) of $PO^{14}C$ and $DO^{14}C$ were calculated from production rates (µmol l^{-1} d^{-1}) by applying Eq. (1). Cell normalised production rates (fmol C $cell^{-1}$ d^{-1}) of pCCHO, HMW-dCCHO and TEP-C were derived from concentrations (µmol C l^{-1}) by applying Eq. (4). Mean values and standard deviations (in parentheses) were derived from sampling 1, 2 and 3 ($\mu = 0.3\,d^{-1}$) and sampling 4, 5 and 6 ($\mu = 0.1\,d^{-1}$), respectively.

μ [d^{-1}]	Treatment	pCCHO [µmol C l^{-1}]	HMW-dCCHO [µmol C l^{-1}]	pCCHO [fmol C $cell^{-1}$ d^{-1}]	HMW-dCCHO [fmol C $cell^{-1}$ d^{-1}]	$PO^{14}C$ [fmol C $cell^{-1}$ d^{-1}]	$DO^{14}C$ [fmol C $cell^{-1}$ d^{-1}]	TEP-C [fmol C $cell^{-1}$]	pCCHO:$PO^{14}C$ [mol % C]	HMW-dCCHO:$DO^{14}C$ [mol % C]
0.3	300-14	32.4 (5.1)	8.3 (1.4)	37.9 (3.7)	10.2 (4.0)	573 (84)	25.3 (2.1)	44.4 (23.6)	6.7 (0.5)	40.0 (14.3)
	550-14	35.8 (6.0)	8.9 (1.8)	36.5 (3.9)	9.1.8 (0.6)	629 (159)	21.1 (10.7)	51.7 (9.8)	6.0 (1.1)	35.0 (4.7)
	900-14	49.3 (15.8)	10.5 (2.0)	47.0 (4.4)	10.3 (1.0)	639 (235)	25.8 (8.6)	31.8 (7.2)	8.1 (3.0)	42.0 (10.6)
	900-18	61.6 (6.8)	11.5 (1.4)	45.8 (3.7)	8.5 (0.4)	566 (116)	20.8 (6.0)	77.1 (6.9)	8.3 (1.9)	43.2 (13.3)
0.1	300-14	69.8 (7.0)	25.8 (1.4)	22.0 (1.6)	8.2 (0.8)	309 (92)	30.3 (10.4)	199.3 (31.7)	7.4 (1.7)	28.7 (7.5)
	550-14	65.9 (5.7)	21.9 (0.3)	22.3 (2.3)	7.4 (0.3)	333 (112)	25.6 (8.2)	196.7 (58.4)	7.2 (2.4)	30.8 (8.7)
	900-14	84.9 (4.1)	19.9 (1.5)	24.5 (4.1)	5.7 (0.7)	253 (16)	30.5 (13.7)	229.9 (74.1)	9.6 (1.0)	21.6 (9.7)
	900-18	82.8 (15.4)	20.7 (2.1)	20.2 (3.5)	5.1 (0.9)	223 (39)	42.8 (6.9)	240.5 (14.4)	9.1 (0.1)	11.9 (0.5)

Table 3. Concentrations (µmol C l^{-1}) of particulate combined carbohydrates (pCCHO) and high molecular weight (>1 kDa) dissolved CCHO (HMW-dCCHO) at various growth-, CO_2 and temperature conditions. Mean values and standard deviations (in parentheses) were derived from sampling 1, 2 and 3 ($\mu = 0.3\,d^{-1}$) and sampling 4, 5 and 6 ($\mu = 0.1\,d^{-1}$), respectively.

μ [d^{-1}]	Sample	Treatment	Fuc [µmol C l^{-1}]		Rha [µmol C l^{-1}]		Ara/GalN [µmol C l^{-1}]		GlcN [µmol C l^{-1}]		Gal [µmol C l^{-1}]		Glc [µmol C l^{-1}]		Man/Xyl [µmol C l^{-1}]		Gal-URA [µmol C l^{-1}]		Glc-URA [µmol C l^{-1}]	
0.3	pCCHO	300-14	0.271	(0.108)	1.070	(0.491)	0.772	(0.095)	0.078	(0.034)	1.894	(0.574)	23.72	(7.16)	0.592	(0.584)	2.704	(0.655)	1.315	(0.381)
		550-14	0.264	(0.218)	0.588	(0.224)	0.801	(0.409)	0.137	(0.090)	1.580	(0.493)	28.52	(3.79)	0.498	(0.308)	2.581	(1.101)	0.786	(0.463)
		900-14	0.346	(0.215)	1.460	(0.896)	0.904	(0.008)	0.042	(0.052)	1.540	(0.601)	41.58	(12.37)	0.914	(0.742)	2.240	(0.618)	0.620	(0.060)
		900-18	0.444	(0.103)	2.210	(0.811)	1.023	(0.367)	0.044	(0.011)	1.855	(0.951)	49.86	(2.66)	2.832	(1.601)	3.779	(0.451)	0.720	(0.366)
0.1	pCCHO	300-14	0.603	(0.139)	2.995	(0.488)	1.560	(0.200)	0.236	(0.021)	3.968	(0.854)	48.62	(2.68)	6.843	(1.838)	4.557	(1.683)	0.587	(0.547)
		550-14	0.495	(0.122)	3.698	(0.428)	1.503	(0.568)	0.193	(0.097)	2.867	(0.350)	44.52	(3.25)	6.006	(1.256)	5.616	(0.601)	0.991	(0.439)
		900-14	0.878	(0.062)	4.270	(0.513)	2.330	(0.340)	0.214	(0.103)	4.809	(0.702)	56.74	(4.32)	7.634	(0.373)	6.512	(0.163)	1.523	(0.126)
		900-18	0.781	(0.036)	1.625	(0.387)	1.956	(0.578)	0.155	(0.081)	2.593	(0.343)	60.17	(9.57)	7.050	(3.501)	7.695	(2.869)	0.803	(0.543)
0.3	HMW-dCCHO	300-14	0.218	(0.048)	0.296	(0.261)	1.579	(0.080)	0.129	(0.050)	0.824	(0.296)	2.066	(0.425)	1.599	(0.331)	0.553	(0.137)	1.066	(0.200)
		550-14	0.206	(0.027)	0.167	(0.045)	1.368	(0.494)	0.082	(0.030)	0.565	(0.367)	2.929	(0.461)	1.686	(0.965)	0.460	(0.277)	1.471	(0.129)
		900-14	0.222	(0.048)	0.371	(0.116)	2.009	(0.669)	0.114	(0.008)	0.601	(0.204)	4.428	(0.928)	1.379	(0.129)	0.543	(0.278)	0.808	(0.125)
		900-18	0.278	(0.052)	0.406	(0.129)	2.211	(0.464)	0.134	(0.053)	0.750	(0.229)	3.862	(0.680)	2.049	(0.365)	0.631	(0.086)	1.155	(0.296)
0.1	HMW-dCCHO	300-14	0.790	(0.012)	1.803	(0.056)	5.280	(0.324)	0.294	(0.014)	2.321	(0.084)	4.142	(0.766)	5.943	(0.222)	3.405	(0.943)	1.856	(0.802)
		550-14	0.723	(0.105)	0.899	(0.152)	4.273	(0.387)	0.290	(0.079)	2.322	(0.079)	6.402	(1.667)	4.604	(0.839)	1.299	(0.159)	1.088	(0.182)
		900-14	0.620	(0.027)	1.414	(0.200)	4.374	(0.263)	0.217	(0.054)	2.027	(0.349)	4.082	(1.404)	4.438	(0.059)	1.613	(0.128)	1.132	(0.193)
		900-18	0.941	(0.346)	0.702	(0.211)	4.776	(0.233)	0.144	(0.016)	2.026	(0.146)	3.588	(0.145)	5.436	(0.775)	2.020	(0.646)	1.070	(0.481)

shifted to the particulate pool with increasing CO_2 and temperature.

As a consequence of the steep rise in HMW-dCCHO at the lower growth rate, the contribution of HMW-dCCHO to tCCHO was significantly higher under enhanced nutrient limitation ($\mu = 0.1\,d^{-1}$) (two way ANOVA, $p = 0.005$). Additionally, the proportion of HMW-dCCHO to tCCHO derived from 300-14 was significantly higher compared to the high CO_2 treatments (900-14 and 900-18, two way ANOVA, Holm-Sidak method, $p \leq 0.004$). While contributions of HMW-dCCHO to tCCHO were clearly higher for 300-14 and 550-14 ($27.1 \pm 2.9\,\%$ and $25.1 \pm 1.3\,\%$) at $\mu = 0.1\,d^{-1}$ compared to those at $\mu = 0.3\,d^{-1}$, proportions were only slightly increasing for 900-14 ($19.3 \pm 1.6\,\%$) and 900-18 ($20.3 \pm 3.4\,\%$) at the lower growth rate (Fig. 2, lower panel) showing a similar partitioning between HMW-dCCHO and pCCHO for these treatments at $\mu = 0.1\,d^{-1}$ as determined for $\mu = 0.3\,d^{-1}$.

Cell normalised pCCHO and HMW-dCCHO production (fmol C $cell^{-1}\,d^{-1}$) was significantly lower at $\mu = 0.1\,d^{-1}$ compared to $\mu = 0.3\,d^{-1}$ (two way ANOVA, Holm-Sidak method, $p < 0.001$). At $\mu = 0.3\,d^{-1}$, cell normalised pCCHO production was higher at elevated CO_2 while no differences between treatments were determined at $\mu = 0.1\,d^{-1}$ (Table 2).

3.4 Carbohydrate composition

Carbohydrate composition was affected by changes in nutrient supply and by varied CO_2 and temperature conditions, albeit to a lesser extent (Fig. 3).

pCCHO was generally dominated by Glc. Averaged for all treatments, Glc comprised $78.9 \pm 8.0\,\%$ of pCCHO at $\mu = 0.3\,d^{-1}$ and $68.1 \pm 3.2\,\%$ at $\mu = 0.1\,d^{-1}$. The decrease in Glc due to the changed growth rate was significant for all treatments (two way ANOVA, $p < 0.001$). Thus, pCCHO composition was shifted to carbohydrates other than Glc, which was significant for Rha ($p \leq 0.015$, except for 300-14 and 900-18), Ara/GalN ($p \leq 0.022$) and Man/Xyl ($p < 0.001$). At $\mu = 0.3\,d^{-1}$, contribution of Rha to pCCHO was in 550-14 and 900-14 significantly higher than in 900-18 ($p \leq 0.003$). Gal contributing to pCCHO was unaffected by changed growth rates but proportions were generally higher in 300-14 than in 900-18 ($p = 0.001$). Contribution of Glc-URA was similar in all treatments with the exception of 300-14 at $\mu = 0.3\,d^{-1}$ ($p \leq 0.008$).

At $\mu = 0.3\,d^{-1}$, carbohydrate contribution to pCCHO declined in the following order: Glc > Gal-URA > Gal > Rha > Glc-URA > Man/Xyl > Ara/GalN > Fuc > GlcN in all treatments. At $\mu = 0.1\,d^{-1}$, composition of pCCHO was clearly shifted to higher proportions of Man/Xyl, being the second most abundant pCCHO after Glc: carbohydrate contribution to pCCHO at $\mu = 0.1\,d^{-1}$ declined in the following order: Glc > Man/Xyl > Gal-URA > Gal > Rha > Ara/GalN > Glc-URA > Fuc > GlcN (Fig. 3).

HMW-dCCHO composition was also significantly affected by changes in nutrient supply ($p < 0.001$) (Fig. 3). From averaged $32.7 \pm 8.9\,\%$ at $\mu = 0.3\,d^{-1}$, contribution of Glc to HMW-dCCHO was reduced to $24.1 \pm 6.6\,\%$ at $\mu = 0.1\,d^{-1}$ ($p < 0.001$). The concomitant increase for HMW-dCCHO monomers contributing to HMW-dCCHO other than Glc was significant for Fuc ($p = 0.002$), Rha ($p = 0.002$, except for 900-18), Ara/GalN ($p \leq 0.006$), Gal ($p \leq 0.014$, except for 300-14), Man/Xyl ($p < 0.001$) and Gal-URA ($p = 0.001$). Contribution of Glc-URA to HMW-dCCHO in all treatments was significantly lower at $\mu = 0.1\,d^{-1}$ ($p \leq 0.015$) except for 900-14. For all treatments at $\mu = 0.3\,d^{-1}$, the contribution of carbohydrate monomers to HMW-dCCHO was in decreasing order: Glc > Ara/GalN > Man/Xyl > Glc-URA > Gal > Gal-URA > Rha > Fuc > GlcN. At $\mu = 0.1\,d^{-1}$, the contribution of carbohydrate monomers was shifted to the following order: Man/Xyl > Ara/GalN > Glc > Gal-URA > Gal > Glc-URA > Rha > Fuc > GlcN. HMW-dCCHO were now dominated by comparable proportions of Man/Xyl, Ara/GalN and Glc with 24.1, 22.1 and 19.8 %, respectively (Fig. 3).

3.5 Transparent exopolymer particles (TEP)

Different nutrient, CO_2 and temperature conditions induced clear changes in the formation of TEP (Fig. 4). At $\mu = 0.1\,d^{-1}$, TEP-C concentrations in all treatments were significantly higher than at $\mu = 0.3\,d^{-1}$ (two way ANOVA, Holm-Sidak method, $p < 0.001$).

At each growth rate, TEP-C was significantly higher in 900-18 than in 300-14 and 550-14 ($p < 0.002$). In accordance with total concentrations of TEP-C (µmol l^{-1}), cell normalised TEP-C (fmol $cell^{-1}$) was significantly higher at $\mu = 0.1\,d^{-1}$ compared to $\mu = 0.3\,d^{-1}$ in all treatments (two way ANOVA, Holm-Sidak method, $p < 0.001$). Cell normalised TEP-C was highest in 900-18 at both growth rates, although not statistically different from values derived from the other treatments ($p = 0.314$) (Table 2). Throughout the experiment, pCCHO significantly correlated with TEP-C (Pearson Product Moment Correlation; $n = 24$, $r^2 = 0.826$, $p < 0.001$) (Fig. 5). Furthermore, concentrations of $DO^{14}C$ (µmol C l^{-1}) also significantly correlated to TEP-C (Pearson Product Moment Correlation; $n = 24$, $r^2 = 0.862$, $p < 0.001$) (Fig. 6). This strongly suggests coherence between the presence of dissolved precursors and TEP. The fact, that higher exudation is not mirrored in higher HMW-dCCHO is most likely reasoned by a transformation of dissolved components into the particulate pool in form of TEP, rich in pCCHO.

The decrease in TEP-C formation (µmol $l^{-1}\,d^{-1}$, derived from Eq. 3) was smaller than the decrease in $PO^{14}C$ production after changing μ from $0.3\,d^{-1}$ to $0.1\,d^{-1}$. Contribution

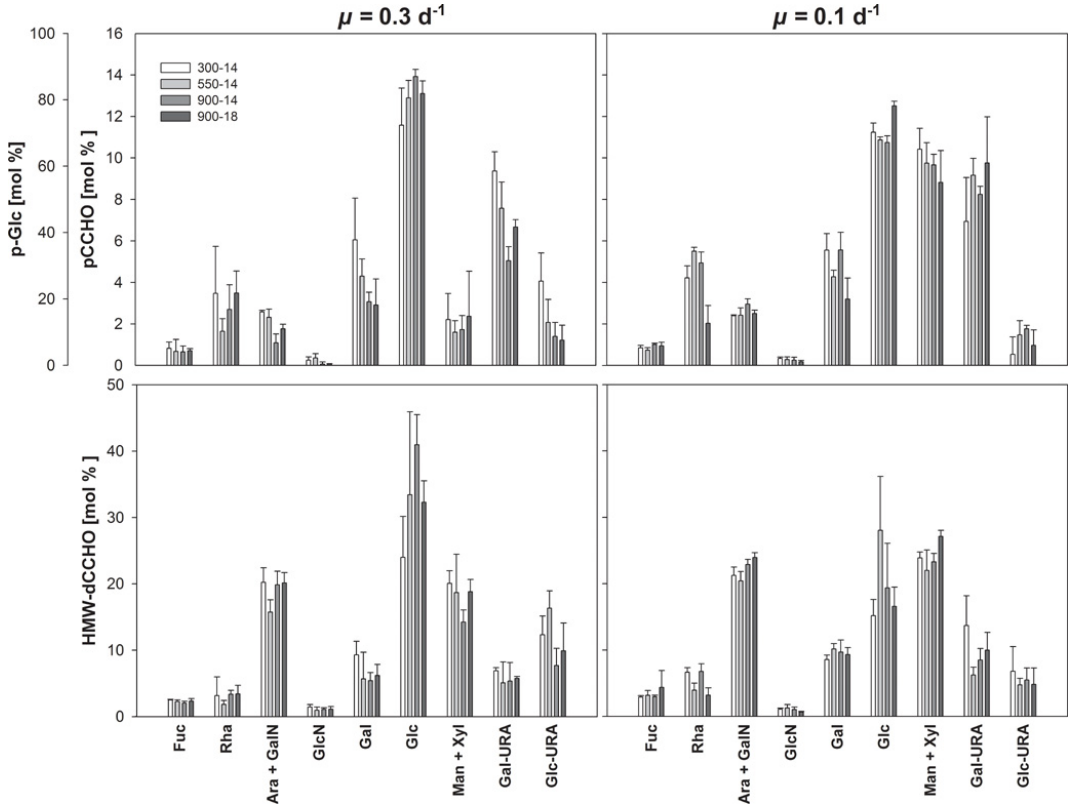

Fig. 3. Composition of particulate combined carbohydrates (pCCHO, upper panels) and high molecular weight (>1 kDa) dissolved CCHO (HMW-dCCHO) (lower panels) at various growth, CO_2 and temperature conditions. Mean values and standard deviations are given as mol % and were derived from sampling 1, 2 and 3 ($\mu = 0.3\,d^{-1}$) and sampling 4, 5 and 6 ($\mu = 0.1\,d^{-1}$), respectively.

of TEP-C to $PO^{14}C$ was, thus, generally higher at enhanced nutrient stress. Averaging for all treatments, TEP-C comprised 2.7 ± 1.4 % of $PO^{14}C$ at $\mu = 0.3\,d^{-1}$ and increased significantly to 8.1 ± 2.7 % at $\mu = 0.1\,d^{-1}$ (two way ANOVA, Holm-Sidak method, $p < 0.001$ (Fig. 7).

Contribution of pCCHO to $PO^{14}C$ was 7.3 ± 1.9 % at $\mu = 0.3\,d^{-1}$ and averaged values increased slightly to 8.4 ± 1.7 % at $\mu = 0.1\,d^{-1}$. Contribution of pCCHO to $PO^{14}C$ were higher at elevated CO_2 (900-14 and 900-18) compared to the 300-14 and 550-14 treatment at both growth rates (Table 2).

The proportion of HMW-dCCHO to $DO^{14}C$ was significantly lower at $\mu = 0.1\,d^{-1}$ (23.2 ± 10.0 %) than at $\mu = 0.3\,d^{-1}$ (40.5 ± 10.5 %) (two way ANOVA, Holm-Sidak method, $p = 0.002$). At $\mu = 0.3\,d^{-1}$, contribution of HMW-dCCHO to $DO^{14}C$ was unaffected by different CO_2 and temperature conditions ($p = 0.664$), and varied between 35.0 % and 43.2 %. At $\mu = 0.1\,d^{-1}$, HMW-dCCHO contribution to $DO^{14}C$ in 900-18 was lowest with 11.9 ± 0.5 % (Fig. 7, Table 2). Thus, high $DO^{14}C$ observed at enhanced nutrient stress were not reflected in HMW-dCCHO. However, low contribution of HMW-dCCHO to $DO^{14}C$ determined for 900-18 was accompanied by highest TEP-C and highest shares of TEP-C contributing to $PO^{14}C$. This suggests a fast partitioning from DOC to POC at elevated CO_2 and temperature (Fig. 7).

4 Discussion

4.1 Particulate and dissolved primary production

In the present experiment, while growth of *E. huxleyi* adapted to the nutrient supply by lowering the growth rate, primary production (PP) and, therefore, the basis for carbon metabolism was clearly decoupled from nutrient assimilation. PP partitioning in dissolved and particulate organic carbon is highly variable, and percentages of extracellular release (PER), depend strongly on environmental conditions that affect the cell's physiology (Myklestad and Haug, 1972; Zlotnik and Dubinsky, 1989; Chen and Wangersky, 1996; Penna et al., 1999; Staats et al., 2000; Wetz and Wheeler, 2003; Magaletti et al., 2004).

During this study, PP of *E. huxleyi* was highest in the 900-18 treatment at $\mu = 0.3\,d^{-1}$ (Fig. 1, upper panel), showing a stimulation of PP by the combined rise of CO_2 and temperature. This is in accordance with earlier findings on the effect of elevated CO_2 (Riebesell et al., 2000) or temperature (Langer et al., 2007) on *E. huxleyi* obtained under nutrient

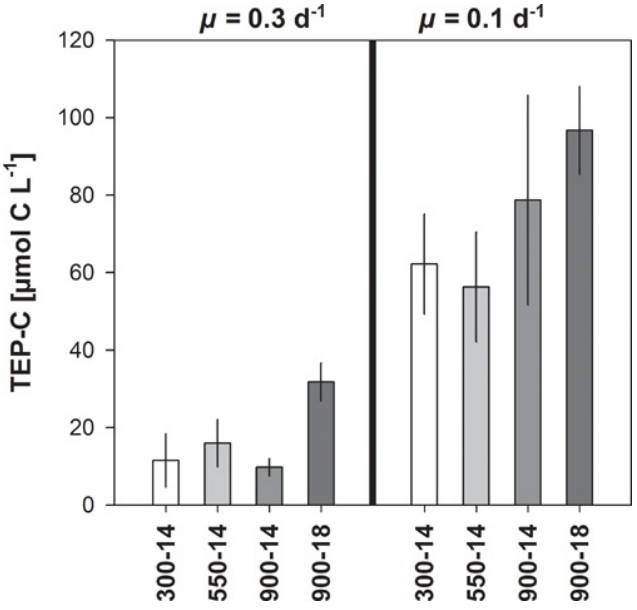

Fig. 4. Concentrations of the carbon content of transparent exopolymer particles (TEP-C) at various growth-, CO_2 and temperature conditions. Mean values and standard deviations were derived from sampling 1, 2 and 3 ($\mu = 0.3\,d^{-1}$) and sampling 4, 5 and 6 ($\mu = 0.1\,d^{-1}$), respectively.

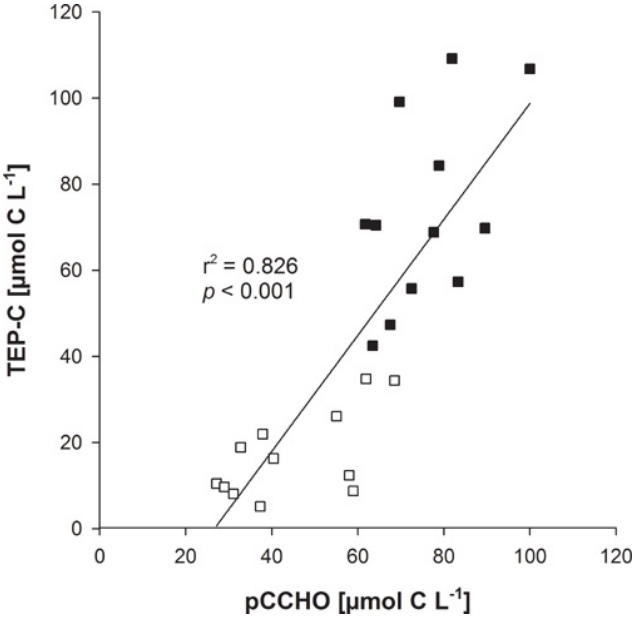

Fig. 5. Correlation between the concentration of particulate combined carbohydrates (pCCHO) and the carbon content of transparent exopolymer particles (TEP-C) (Pearson Product Moment Correlation; $n = 24$, $r^2 = 0.826$, $p < 0.001$). Open and closed symbols represent data obtained at $\mu = 0.3\,d^{-1}$ and $\mu = 0.1\,d^{-1}$, respectively.

replete conditions. If nutrients are abundant, a linear relationship between PP and extracellular release (ER) is gener-

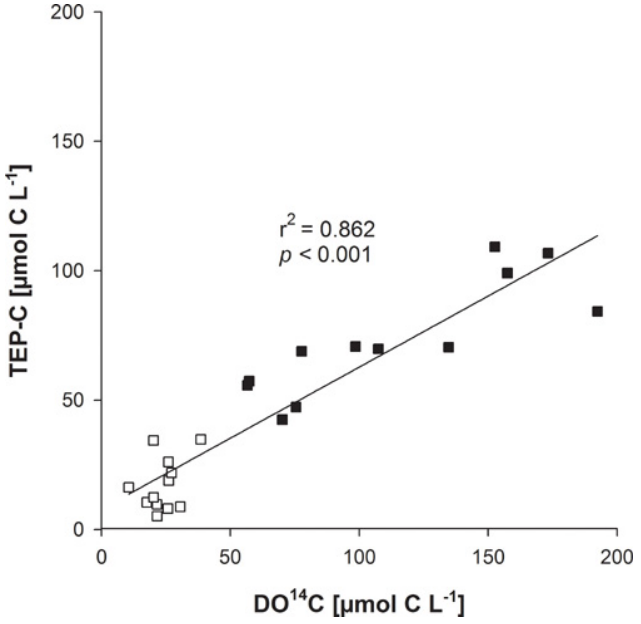

Fig. 6. Correlation between the concentration of dissolved organic carbon ($DO^{14}C$, μmol C L^{-1}, derived from Eq. 1) and the carbon content of transparent exopolymer particles (TEP-C) (Pearson Product Moment Correlation; $n = 24$, $r^2 = 0.862$, $p < 0.001$). Open and closed symbols represent data obtained at $\mu = 0.3\,d^{-1}$ and $\mu = 0.1\,d^{-1}$, respectively.

ally assumed (Zlotnik and Dubinsky, 1989; Baines and Pace, 1991; Verity et al., 1991). Nutrient limitation, however, was regularly shown to decouple PP and ER, resulting in higher PER due to a strong relative increase in ER (Myklestad, 1977; Obernosterer and Herndl, 1995; Staats et al., 2000; López-Sandoval et al., 2011). While high light intensities and CO_2 stimulate carbon assimilation (e.g., primary production) nutrient limitation hampers cell division and growth at the same time (Fogg, 1966; Baines and Pace, 1991; Banse, 1994). A particular increase in carbon assimilation relative to the uptake of N and P is referred to as carbon overconsumption (Toggweiler, 1993; Schartau et al., 2007). Carbon overconsumption susceptibly alters the stoichiometric relation between major elements and large deviations from Redfield's C:N:P of 106:16:1 were regularly observed in the field (Fraga, 2001; Geider and LaRoche, 2002) as well as in laboratory experiments (Sciandra et al., 2003; Leonardos and Geider, 2005).

The present experiment was designed to investigate the combined effect of nutrient limitation (e.g., phosphorus limitation), CO_2 and temperature on organic carbon production at two low growth rates. In agreement with earlier findings, higher PER was determined at conditions of enhanced nutrient stress after changing the nutrient supply rate from $D = 0.3\,d^{-1}$ to $D = 0.1\,d^{-1}$. A direct relationship between PER and growth rate was questioned (Williams, 1990), primarily following a chemostat study with *Thalassiosira pseudonana*

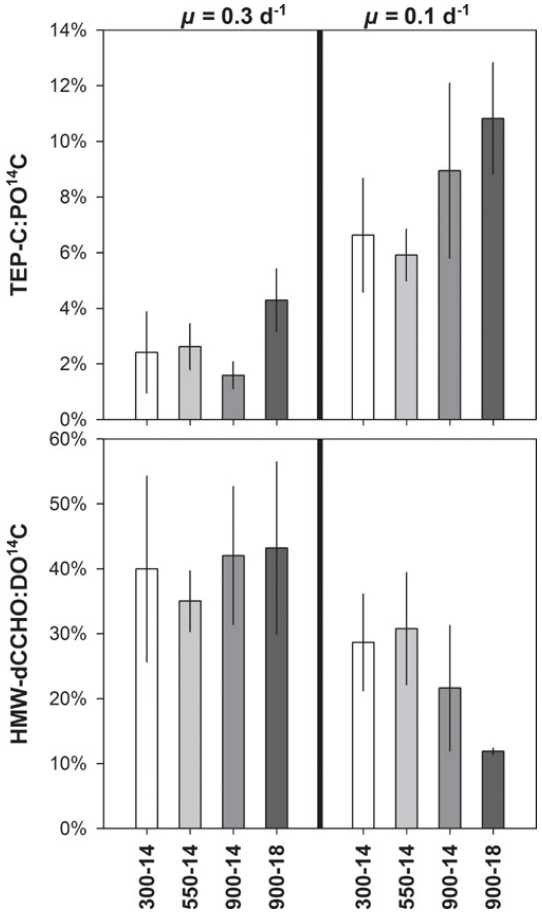

Fig. 7. Carbon partitioning. Contribution (mol % C) of the carbon content of transparent exopolymer particles (TEP-C) to particulate organic carbon ($PO^{14}C$), (upper panel) and of high molecular weight (>1 kDa) dissolved CCHO (HMW-dCCHO) to dissolved organic carbon ($DO^{14}C$, µmol C l^{-1}) various growth-, CO_2 and temperature conditions. Mean values and standard deviations were derived from sampling 1, 2 and 3 ($\mu = 0.3\,d^{-1}$) and sampling 4, 5 and 6 ($\mu = 0.1\,d^{-1}$), respectively. Concentrations (µmol l^{-1}) of $PO^{14}C$ and $DO^{14}C$ were calculated from production rates (µmol l^{-1} d^{-1}) by applying Eq. (1).

(diatom) (Smith and Platt, 1984) exhibiting very low PER varying in a range of 1.2–2.7 % at growth rates between 0.29 and 2.50 d^{-1}. Data obtained here, however, showed a strong impact of growth rate as a result of enhanced nutrient limitation on PER, which was obvious in the pronounced increase of PER from averaged 3.7 % at $\mu = 0.3\,d^{-1}$ to 11.0 % at $\mu = 0.1\,d^{-1}$ (Fig. 1, lower panel). Since the reduction in growth rate is a result of enhanced nutrient limitation, data presented here are in accordance with a variety of studies reporting on higher PER with increasing nutrient limitation (Myklestad, 1977; Obernosterer and Herndl, 1995; López-Sandoval et al., 2011).

The effect of elevated CO_2 and temperature on phytoplankton exudation, however, has not yet been directly tested, but ER of organic molecules was hypothesised to be stimulated by either elevated CO_2 (Engel, 2002) or by elevated temperature (Moran et al., 2006; Wohlers et al., 2009; Engel et al., 2011). In the present study, both, PP and ER showed an increasing trend with elevated CO_2 and temperature at a growth rate of $\mu = 0.3\,d^{-1}$ (Fig. 1), and the coupling of PP and ER, thus, yielded comparable PER in all treatments. At enhanced nutrient stress ($\mu = 0.1\,d^{-1}$) the CO_2 and temperature effect on POC production was diminished (Fig. 1, upper panel). DOC production, however, was clearly stimulated by the combined effect of enhanced nutrient limitation and elevated CO_2 and temperature (Fig. 1, middle panel). Organic carbon production was, thus, shifted to the dissolved pool at greenhouse conditions, yielding highest PER of 16.3 % (Fig. 1, lower panel). At severe nutrient stress, ER is, therefore, most likely of greater importance for the carbon partitioning because the reduction of POC production coincides with an enhancement of DOC production. For the future ocean, this implies a potential decoupling of growth, POC production and DOC production.

In natural systems, freshly produced DOC is readily taken up by heterotrophic bacteria (Azam et al., 1983; Martin et al., 1987). Elevated temperature as well as decreased pH has been shown to accelerate enzymatic reactions and to enhance bacterial degradation in marine systems especially concerning protease, and α- and β-glucosidase activity (Grossart et al., 2006; Piontek et al., 2009, 2010). Yamada and Suzumura (2010) reported that bacterial β-glucosidase activity is unaffected by ocean acidification and amino peptidase activity even decreased at lowered pH. A recent publication by Endres et al. (2012) however, supported the hypothesis on stimulated bacterial enzyme activity under future ocean conditions by reporting on an increased amino peptidase activity in autotrophic cyanobacteria. Phytoplankton exudates derived under phosphorus limitation, however, may in general not be efficiently utilised by heterotrophic bacteria. This was either argued by a severe slowing down of bacterial metabolism due to limiting inorganic and organic phosphorus concentrations (Obernosterer and Herndl, 1995), or by the recalcitrant characteristics of DOC released from phytoplankton under phosphorus limitation (Puddu et al., 2003). A loss of DOC due to heterotrophic activity might, thus, be minimised and carbon overconsumption and excess exudation may result in higher concentrations of DOC in the future ocean.

4.2 Carbohydrates and linkages to TEP-formation

Concentrations of HMW-dCCHO, pCCHO and TEP-C were higher in all treatments under enhanced nutrient limitation ($\mu = 0.1\,d^{-1}$). Specific production rates of CCHO reached physiological steady states for each D, albeit, decoupled from cell growth, resulting in different yields for $\mu = 0.3\,d^{-1}$ and $\mu = 0.1\,d^{-1}$, respectively. Relative to the growth rate, specific production of carbohydrate-rich compounds was generally higher at $\mu = 0.1\,d^{-1}$, resulting in higher

concentrations of all carbon rich compounds. The different yields of organic carbon in form of carbohydrates and TEP-C were thus not related to the cell density of *E. huxleyi*, but clearly due to changed specific production (Figs. 2 and 4).

A stronger partitioning of PP to the dissolved pool may reduce carbon export in the future ocean if DOC is not transferred to the particulate pool via aggregation processes (Kim et al., 2011). Phytoplankton exudation, however, does not only increase DOC concentration, it also provides the precursors for the formation of transparent exopolymer particles (TEP) by physical coagulation (Passow, 2000). This abiotic formation of particles such as TEP from organic molecules was proposed to be a major mechanism for the loss of dissolved carbohydrates in the ocean (Skoog and Benner, 1997; Engel et al., 2004b). A recent publication by Passow (2012) showed that the abiotic TEP formation, i.e., the coagulation process itself, is not impacted by changes in pH. Here we report on the biological production of dissolved precursors and the subsequent production of TEP that was significantly related to PER (Fig. 6). The composition of dissolved carbohydrates was significantly affected by varied conditions of nutrient supply while the influence of CO_2 and T was negligible (Fig. 3). PER in all treatments was higher at $\mu = 0.1\,d^{-1}$ compared to $\mu = 0.3\,d^{-1}$ and highest exudation was clearly determined for the cells grown at elevated CO_2 and temperature (Fig. 1). The higher TEP formation observed at 900-18 is, therefore, a likely result of higher concentrations of precursors due to enhanced biological activity, rather than the quality of dissolved material. For the present study, the steep rise in PER, as a consequence of changed nutrient supply, CO_2 and temperature, was not mirrored in the proportion of HMW-dCCHO contributing to $DO^{14}C$ (Fig. 7, lower panel) and of HMW-dCCHO to tCCHO (Fig. 2, lower panel). The TEP-C:$PO^{14}C$ ratio, however, (Fig. 7, upper panel) resembles the PER. A significant correlation between the concentration of dissolved precursors ($DO^{14}C$, µmol C l^{-1}), and TEP-C (µmol C l^{-1}) was determined ($r^2 = 0.862$, $p < 0.001$, Fig. 6). The transfer of HMW-dCCHO (low HMW-dCCHO:$DO^{14}C$) and the concomitant relative increase in pCCHO (low HMW-dCCHO:pCCHO) was accompanied by an increase in TEP-C (high TEP-C:$PO^{14}C$) (Figs. 4 and 7). These finding, therefore, indicate a fast transformation of HMW-dCCHO to pCCHO in form of TEP, which was most pronounced at elevated CO_2 and temperature at enhanced nutrient stress.

Results obtained during this study, thus, strongly support the idea of a direct pathway between DOC in form of HMW-dCCHO and POC by physical aggregation, as suggested previously (Chin et al., 1998; Wells, 1998; Engel et al., 2004b; Verdugo et al., 2004; Verdugo et al., 2008; Ding et al., 2009) and shows, that this pathway will be of greater importance under conditions of simultaneously increased CO_2 and temperature. The hypothesis of a direct transfer of HMW-dCCHO to TEP is additionally supported by a significant correlation between pCCHO and TEP-C concentration ($r^2 = 0.826$, $p < 0.001$) (Fig. 5).

Compared to $\mu = 0.3\,d^{-1}$, HMW-dCCHO composition at $\mu = 0.1\,d^{-1}$ was shifted to comparable contributions of Man/Xyl, Ara/GalN and Glc accompanied by high contributions of Glc, Man/Xyl and Gal-URA to pCCHO and an increase in TEP (Figs. 3 and 4 and Table 3). Compared to other carbohydrate monomers, this indicates a higher relative increase of the production and exudation of Man/Xyl and Gal-URA at excess nutrient limitation. Throughout the experiment for all treatments, concentrations of particulate Gal-URA, an acidic sugar which is typical for *E. huxleyi* (Nanninga et al., 1996), correlated significantly with concentrations of TEP-C ($r^2 = 0.827$, $p < 0.001$). Low contributions of HMW-dCCHO to pCCHO despite the high ER, can be explained by a transfer from neutral (Man/ Xyl) and acidic HMW-dCCHO (Gal-URA) to higher proportions of neutral and acidic pCCHO as a characteristic fraction of TEP (Skoog et al., 2008). Therefore, data obtained here show coherence between enhanced exudation of DOC and higher concentrations of pCCHO and TEP-C. A significant proportion of DOC (up to 90 %) derived from phytoplankton exudation was shown to be comprised by carbohydrates (Myklestad, 1995). Here, HMW-dCCHO comprised 12 to 43 % of freshly produced DOC (Fig. 7) and the comparably low proportions further indicate the transfer of HMW-dCCHO to POC due to aggregation processes in accordance to the model proposed by Engel et al. (2004b) (Figs. 2, 6 and 7).

Earlier studies with *E. huxleyi* reported that TEP-C accounted for 63 % of POC (Engel et al., 2004a) during a mesocosm experiment. In the Bay of Biscay, Harlay et al. (2009) observed a 12 % contribution of TEP-C to POC during a bloom of coccolithophores, dominated by *E. huxleyi*. During this study, TEP-C explained on average 3 % at $\mu = 0.3\,d^{-1}$ and 8 % at $\mu = 0.1\,d^{-1}$ of POC with highest proportions of TEP-C contributing to POC observed in the 900-18 treatment.

Thus, compared to field and mesocosm systems, the contribution of TEP-C to POC was relatively low during this chemostat experiment. This suggests that physiological non-steady state situations, such as occurring naturally during bloom situations, have a different impact than conditions of steady-state growth. Clearly, more information on loss processes of TEP in marine systems is needed to evaluate the role of TEP for carbon partitioning in the future ocean.

5 Conclusions

Emiliania huxleyi is one of the most abundant coccolithophore in the global ocean and despite its small size an important contributor to marine primary production. Significantly higher cell densities and, therefore, minimised cell quota for phosphorus were exclusively induced by elevated CO_2 (Borchard et al., 2011). Sustaining photosynthesis and

growth, while increasing DOC production, potentially represents a physiological strategy allowing (1) the production of high biomass at high CO_2 on low nutrient supply and (2) a quick response of cellular processes when nutrients become available again.

Data presented here reveal that nutrient concentration had the strongest impact on organic carbon partitioning, relative to the influence of CO_2 and temperature. DOC and POC production could, therefore, be more affected in the future ocean by changed nutrient or growth conditions, either on a regional basis or during the seasonal succession. Our data further imply that partitioning of organic carbon production to the dissolved pool will most likely be additionally promoted at elevated CO_2 and temperature. This, however, will depend on the synergistic effect of nutrient limitation and elevated CO_2 and temperature on P quota, cell size and carbon overconsumption.

Despite the fact, that DOC itself does not sink, an enhanced DOC pool most likely provides higher concentrations of precursor material in form of HMW-dCCHO for aggregation processes. Although only slightly affected by elevated CO_2, the composition of HMW-dCCHO could be relevant for an efficient transfer of HMW-dCCHO to the particulate pool. However, TEP-formation in the greenhouse ocean seems to be primarily driven by the higher concentration of precursor material due to higher exudation.

The importance of TEP as part of the POC pool is well acknowledged in studies of organic carbon fluxes (Engel and Passow, 2001; Mari et al., 2001; Engel et al., 2004b; Arrigo, 2007; De La Rocha and Passow, 2007; Schartau et al., 2007; Verdugo et al., 2008). A quantitative and qualitative connection between DOC production and TEP-C formation as shown for the present study was proposed earlier (Jackson and Burd, 1998; Engel et al., 2004b). However, timing of the biological process of extracellular release and the abiotic formation of particles may potentially be decoupled. Low HMW-dCCHO concentrations contributing to tCCHO at high exudation rates may, thus, point to a fast aggregation of DOC into TEP. Since precursors in form of dissolved CCHO are effectively reduced at elevated CO_2 and temperature, data obtained from this experimental study suggest, that TEP-formation occurs faster at elevated temperature most likely due to physical and chemical processes (McCave, 1984; Claquin et al., 2008). However, the quantitative importance of TEP contributing to the POC pool in the future ocean needs further studies taking into account the multiple factors and processes occurring in natural ecosystems.

Acknowledgements. This study was supported by the Helmholtz Association (HZ-NG-102) and the BMBF project BIOACID (funding reference no. 03F0608B). This work is also a contribution to the "European Project on Ocean Acidification" (EPOCA) which received funding from the European Community's Seventh Framework Programme (FP7/2007-2013) under grant agreement no. 211384. Nicole Händel and Judith Piontek are gratefully acknowledged for constructive comments and discussions on the manuscript.

Edited by: C. Klaas

References

Arrigo, K. R.: Carbon cycle – Marine manipulations, Nature, 450, 491–492, 2007.

Azam, F., Fenchel, T., Field, J. G., Gray, J. S., Meyer-Reil, L. A., and Thingstad, F.: The ecological role of water-column microbes in the sea, Marine Ecology Progress Series, 10, 257–263, 1983.

Baines, S. B. and Pace, M. L.: The production of dissolved organic matter by phytoplankton and its importance to bacteria: Patterns across marine and freshwater systems, Limnol. Oceanogr., 36, 1078–1090, 1991.

Banse, K.: Uptake of inorganic carbon and nitrate by marine plankton and the Redfield ratio, Global Biogeochem. Cycles, 8, 81–84, 1994.

Biddanda, B. and Benner, R.: Carbon, nitrogen, and carbohydrate fluxes during the production of particulate and dissolved organic matter by marine phytoplankton, Limnol. Oceanogr., 42, 506–518, 1997.

Borchard, C., Borges, A. V., Händel, N., and Engel, A.: Biogeochemical response of *Emiliania huxleyi* (PML B92/11) to elevated CO_2 and temperature under phosphorous limitation: a chemostat study, J. Experimental Marine Biology and Ecology, 410, 61–71, 2011.

Boyd, P. W. and Doney, S. C.: Modelling regional responses by marine pelagic ecosystems to global change, Geophys. Res. Lett., 29, 1806–1810, 2002.

Caldeira, K.: What Corals are Dying to Tell Us About CO_2 and Ocean Acidification, Oceanography, 20, 188–195, 2007.

Caldeira, K. and Wickett, M. E.: Anthropogenic carbon and ocean pH, Nature, 425, 365–365, 2003.

Chen, W. H. and Wangersky, P. J.: Production of dissolved organic carbon in phytoplankton cultures as measured by high-temperature catalytic oxidation and ultraviolet photo-oxidation methods, J. Plankton Res., 18, 1201–1211, 1996.

Chin, W.-C., Orellana, M., and Verdugo, P.: Spontaneous assembly of marine dissolved organic matter into polymer gels, Nature, 391, 568–572, 1998.

Chisholm, S. W.: Oceanography: Stirring times in the Southern Ocean, Nature, 407, 685–687, 2000.

Claquin, P., Probert, I., Lefebvre, S., and Veron, B.: Effects of temperature on photosynthetic parameters and TEP production in eight species of marine microalgae, Aquatic Microbial Ecology, 51, 1–11, 2008.

De Jong, E., van Rens, L., Westbroek, P., and Bosch, L.: Biocalcification by the marine alga *Emiliania huxleyi* (Lohmann) Kamptner, European Journal of Biochemistry, 99, 559–567, 1979.

De La Rocha, C. L. and Passow, U.: Factors influencing the sinking of POC and the efficiency of the biological carbon pump, Deep-Sea Res. Part Ii-Topical Studies in Oceanography, 54, 639–658, 2007.

Delille, B., Harlay, J., Zondervan, I., Jacquet, S., Chou, L., Wollast, R., Bellerby, R., Frankignoulle, M., Borges, A., Riebesell, U., and Gattuso, J.: Response of primary production and calcification to changes of pCO_2 during experimental blooms of the coccol-

ithophorid *Emiliania huxleyi*, Global Biogeochem. Cycles, 19, GB2023, doi:10.1029/2004GB002318, 2005.

Descy, J. P., Leporcq, B., Viroux, L., Francois, C., and Servais, P.: Phytoplankton production, exudation and bacterial reassimilation in the River Meuse (Belgium), J. Plankton Res., 24, 161–166, 2002.

Ding, Y. X., Hung, C. C., Santschi, P. H., Verdugo, P., and Chin, W. C.: Spontaneous assembly of exopolymers from phytoplankton, Terrestrial Atmospheric and Oceanic Sciences, 20, 741–747, 2009.

Ducklow, H., Carlson, C., Church, M., Kirchman, D., Smith, D., and Steward, G.: The seasonal development of the bacterioplankton bloom in the Ross Sea, Antarctica 1994–1997, Deep-Sea Res. Part II – Topical Studies in Oceanography, 48, 4199–4221, 2001.

Egge, J. K. and Heimdal, B. R.: Blooms of phytoplankton including *Emiliania huxleyi* (haptophyta) – effects of nutrient supply in different n:P ratios, Sarsia, 79, 333–348, 1994.

Egge, J. K., Thingstad, T. F., Larsen, A., Engel, A., Wohlers, J., Bellerby, R. G. J., and Riebesell, U.: Primary production during nutrient-induced blooms at elevated CO_2 concentrations, Biogeosciences, 6, 877–885, doi:10.5194/bg-6-877-2009, 2009.

Endres, S., Unger, J., Wannicke, N., Nausch, M., Voss, M., and Engel, A.: Response of *Nodularia spumigena* to pCO_2 – Part 2: Exudation and extracellular enzyme activities, Biogeosciences Discuss., 9, 5109–5151, doi:10.5194/bgd-9-5109-2012, 2012.

Engel, A.: Direct relationship between CO_2 uptake and transparent exopolymer particles production in natural phytoplankton, J. Plankton Res., 24, 49–53, 2002.

Engel, A. and Händel, N.: A novel protocol for determining the concentration and composition of sugars in particulate and in high molecular weight dissolved organic matter (HMW-DOM) in seawater, Marine Chemistry, 127, 180–191, 2011.

Engel, A. and Passow, U.: Carbon and nitrogen content of transparent exopolymer particles (TEP) in relation to their Alcian Blue adsorption, Marine Ecology-Progress Series, 219, 1–10, 2001.

Engel, A., Delille, B., Jacquet, S., Riebesell, U., Rochelle-Newall, E., Terbrüggen, A., and Zondervan, I.: Transparent exopolymer particles and dissolved organic carbon production by *Emiliania huxleyi* exposed to different CO_2 concentrations: a mesocosm experiment, Aquatic Microbial Ecology, 34, 93–104, 2004a.

Engel, A., Thoms, S., Riebesell, U., Rochelle-Newall, E., and Zondervan, I.: Polysaccharide aggregation as a potential sink of marine dissolved organic carbon, Nature, 428, 929–932, 2004b.

Engel, A., Händel, N., Wohlers, J., Lunau, M., Grossart, H.-P., Sommer, U., and Riebesell, U.: Effects of sea surface warming on the production and composition of dissolved organic matter during phytoplankton blooms: results from a mesocosm study, J. Plankton Res., 33, 357–372, 2011.

Falkowski, P. G.: The role of phytoplankton photosynthesis in global biogeochemical cycles, Photosynthesis Res., 39, 235–258, 1994.

Falkowski, P., Scholes, R. J., Boyle, E., Canadell, J., Canfield, D., Elser, J., Gruber, N., Hibbard, K., Hogberg, P., Linder, S., Mackenzie, F. T., Moore, B., Pedersen, T., Rosenthal, Y., Seitzinger, S., Smetacek, V., and Steffen, W.: The global carbon cycle: A test of our knowledge of earth as a system, Science, 290, 291–296, 2000.

Feng, Y., Warner, M. E., Zhang, Y., Sun, J., Fu, F. X., Rose, J. M., and Hutchins, D. A.: Interactive effects of increased pCO_2, temperature and irradiance on the marine coccolithophore *Emiliania huxleyi* (Prymnesiophyceae), European Journal of Phycology, 43, 87–98, 2008.

Fichtinger Schepman, A. M. J., Kamerling, J. P., Vliegenthart, J. F. G., De Jong, E. W., Bosch, L., and Westbroek, P.: Composition of a methylated, acidic polysaccharide associated with coccoliths of *Emiliania huxleyi* (Lohmann) Kampner, Carbohydrate Res., 69, 181–189, 1979.

Fogg, G. E.: The extracellular products of algae, Oceanogr. Marine Biology: Annual Review, 4, 195–212, 1966.

Fogg, G. E.: The ecological significance of extracellular products of phytoplankton photosynthesis, Botanica Marina, 26, 3–14, 1983.

Fraga, F.: Phytoplanktonic biomass synthesis: application to deviations from Redfield stoichiometry, Scientia Marina, 65, 153–169, 2001.

Gargas, E.: A Manual for Phytoplankton Primary Production Studies in the Baltic, The Baltic Marine Biologists, 2, 88 p., 1975.

Geider, R. J. and LaRoche, J.: Redfield revisited: variability of C:N:P in marine microalgae and its biochemical basis, European Journal of Phycology, 37, 1–17, 2002.

Godoi, R. H. M., Aerts, K., Harlay, J., Kaegi, R., Ro, C. U., Chou, L., and Van Grieken, R.: Organic surface coating on coccolithophores – *Emiliania huxleyi*: Its determination and implication in the marine carbon cycle, Microchemical Journal, 91, 266–271, 2009.

Gogou, A. and Repeta, D. J.: Particulate-dissolved transformations as a sink for semi-labile dissolved organic matter: Chemical characterization of high molecular weight dissolved and surface-active organic matter in seawater and in diatom cultures, Marine Chemistry, 121, 215–223, 2010.

Gran, G.: Determination of the equivalence point in potentiometric titrations of seawater with hydrochloric acid, Oceanology Acta, 5, 209–218, 1952.

Grasshoff, K., Kremeling, K., and Ehrhardt, M.: Methods of seawater analysis; Third, completely revised and extended edition, Wiley-VHC, 1999.

Grossart, H. P., Allgaier, M., Passow, U., and Riebesell, U.: Testing the effect of CO_2 concentration on the dynamics of marine heterotrophic bacterioplankton, Limnol. Oceanogr., 51, 1–11, 2006.

Guillard, R. R. L. and Ryther, J. H.: Studies of marine planktonic diatoms. I. *Cyclotella nana* Hustedt and *Detonula confervacea* Cleve, Can. J. Microbiology, 8, 229–239, 1962.

Harlay, J., De Bodt, C., Engel, A., Jansen, S., d'Hoop, Q., Piontek, J., Van Oostende, N., Groom, S., Sabbe, K., and Chou, L.: Abundance and size distribution of transparent exopolymer particles (TEP) in a coccolithophorid bloom in the northern Bay of Biscay, Deep-Sea Res. Part I-Oceanographic Research Papers, 56, 1251–1265, 2009.

Head, R. N., Crawford, D. W., Egge, J. K., Harris, R. P., Kristiansen, S., Lesley, D. J., Maranon, E., Pond, D., and Purdie, D. A.: The hydrography and biology of a bloom of the coccolithophorid *Emiliania huxleyi* in the northern north sea, J. Sea Res., 39, 255–266, 1998.

Ittekkot, V., Brockman, U., Michaelis, W., and Degens, E. T.: Dissolved free and combined carbohydrates during a phytoplankton bloom in the Northern North Sea, Marine Ecology Progress Series, 299–305, 1981.

Jackson, G. and Burd, A.: Aggregation in the marine environment, Environ. Sci. Tech., 32, 2805–2814, 1998.

Kaehler, P., Bjørnsen, P. K., Lochte, K., and Antia, A. S.: Dissolved organic matter and its utilization by bacteria during spring in the Southern Ocean, Deep-Sea Res. Part II – Topical Studies in Oceanography, 44, 341-353, 1997.

Karl, D. M., Hebel, D. V., Bjorkman, K., and Letelier, R. M.: The role of dissolved organic matter release in the productivity of the oligotrophic North Pacific Ocean, Limnol. Oceanogr., 43, 1270–1286, 1998.

Karl, D. M., Bidigare, R. R., and Letelier, R. M.: Long-term changes in plankton community structure and productivity in the North Pacific Subtropical Gyre: The domain shift hypothesis, Deep-Sea Res. Part II – Topical Studies in Oceanography, 48, 1449–1470, 2001.

Kayano, K. and Shiraiwa, Y.: Physiological regulation of coccolith polysaccharide production by phosphate availability in the coccolithophorid *Emiliania huxleyi*, Plant Cell Physiol., 50, 1522–1531, 2009.

Kim, J. M., Lee, K., Shin, K., Yang, E. J., Engel, A., Karl, D. M., and Kim, H. C.: Shifts in biogenic carbon flow from particulate to dissolved forms under high carbon dioxide and warm ocean conditions, Geophys. Res. Lett., 38, L08612, doi:10.1029/2011GL047346, 2011.

Koroleff, F. and Grasshoff, K.: Determination of nutrients, in: Methods of Seawater Analysis, edited by: Grasshoff, K., Ehrhardt, M., and Kremling, K., Verlag Chemie, Weinheim, 419 p., 1983

Lancelot, C.: Extracellular release of small and large molecules by phytoplankton in the Southern bight of the North Sea, Estuar. Coastal Shelf Sci., 18, 65–77, 1984.

Langer, G., Gussone, N., Nehrke, G., Riebesell, U., Eisenhauer, A., and Thoms, S.: Calcium isotope fractionation during coccolith formation in *Emiliania huxleyi*: Independence of growth and calcification rate, Geochemistry Geophysics Geosystems, 8, Q05007, doi:10.1029/2006GC001422, 2007.

Langer, G., Nehrke, G., Probert, I., Ly, J., and Ziveri, P.: Strain-specific responses of Emiliania huxleyi to changing seawater carbonate chemistry, Biogeosciences, 6, 2637–2646, doi:10.5194/bg-6-2637-2009, 2009.

Lee, S. and Fuhrman, J. A.: Relationships between biovolume and biomass of naturally derived marine bacterioplankton, Applied Environ. Microbiol., 53, 1298–1303, 1987.

Leonardos, N. and Geider, R. J.: Elevated atmospheric carbon dioxide increases organic carbon fixation by *Emiliania huxleyi* (Haptophyta), under nutrient-limited high-light conditions, J. Phycology, 41, 1196–1203, 2005.

Lewis, E. and Wallace, D.: Program Developed for CO_2 System Calculations. ORNL/CDIAC-105, Carbon Dioxide Information Analysis Center, Oak Ridge National Laboratory, US Department of Energy, Oak Ridge, Tennessee, 1998.

López-Sandoval, D. C., Fernández, A., and Marañón, E.: Dissolved and particulate primary production along a longitudinal gradient in the Mediterranean Sea, Biogeosciences, 8, 815–825, doi:10.5194/bg-8-815-2011, 2011.

Magaletti, E., Urbani, R., Sist, P., Ferrari, C. R., and Cicero, A. M.: Abundance and chemical characterization of extracellular carbohydrates released by the marine diatom Cylindrotheca fusiformis under N- and P-limitation, European Journal of Phycology, 39, 133–142, 2004.

Mague, T. H., Friberg, E., Hughes, D. J., and Morris, I.: Extracellular release of carbon by marine phytoplankton; a physiological approach, Limnol. Oceanogr., 25, 262–279, 1980.

Mari, X., Beauvais, S., Lemée, R., and Pedrotti, M. L.: Non-Redfield C:N ratio of transparent exopolymeric particles in the northwestern Mediterranean Sea, Limnol. Oceanogr., 46, 1831–1836, 2001.

Martin, J. H., Knauer, G. A., Karl, D. M., and Broenkow, W. W.: VERTEX – Carbon cycling in the northeast pacific, Deep-Sea Res. Part I – Oceanographic Research Papers, 34, 267–285, 1987.

McCave, I. N.: Size spectra and aggregation of suspended particles in the deep ocean, Deep-Sea Res., 31, 329–352, 1984.

Meehl, G., Stocker, T., Collins, W., Friedlingstein, P., Gaye, A., Gregory, J., Kitoh, A., Knutti, R., Murphy, J., Noda, A., Raper, S., Watterson, I., Weaver, A., and Zhao, Z.-C.: Global Climate Projections, in: Climate Change 2007: The Physical Science Basis. Contribution of Working Group I to the Fourth Assessment Report of the Intergovernmental Panel on Climate Change, 2007.

Mopper, K., Zhou, J. A., Ramana, K. S., Passow, U., Dam, H. G., and Drapeau, D. T.: The role of surface-active carbohydrates in the flucculation of a diatom bloom in a mesocosm, Deep-Sea Res. Part II – Topical Studies in Oceanography, 42, 47–73, 1995.

Moran, X. A. G., Sebastian, M., Pedros-Alio, C., and Estrada, M.: Response of Southern Ocean phytoplankton and bacterioplankton production to short-term experimental warming, Limnol. Oceanogr., 51, 1791–1800, 2006.

Myklestad, S.: Production of carbohydrates by marine phytoplanktonic diatoms. Influence of N-P ratio in growth medium on assimilation ratio, growth rate and production of cellular and extracellular carbohydrates by *Chaetoceros affinis var willei* (Gran) husted and *Sceletonema costatum* (Grev) cleve, J. Experimental Marine Biology and Ecology, 29, 161–179, 1977.

Myklestad, S. M.: Release of extracellular products by phytoplankton with special emphasis on polysaccharides, Sci. Total Environ., 165, 155–164, 1995.

Myklestad, S. and Haug, A.: Production of carbohydrates by the marine diatom *Chaetoceros affinis* var Willei (Gran) Hustedt I, in: Effect of the concentration of nutrients in the culture medium, , J. Experimental Marine Biology and Ecology, 9, 125–136, 1972.

Myklestad, S., Holm-Hansen, O., Varum, K. M., and Volcani, B. E.: Rate of release of extracellular amino-acids and carbohydrates from the marine diatom *Chaetoceros affinis*, J. Plankton Res., 11, 763–773, 1989.

Nagata, T.: Production mechanisms of dissolved matter, in: Microbial Ecology of the Oceans, edited by: Kirchmann, D. L., Wiley-Liss, New York, pp. 121–152, 2000.

Nanninga, H. J., Ringenaldus, P., and Westbroek, P.: Immunological quantitation of a polysaccharide formed by *Emiliania huxleyi*, J. Marine Syst., 9, 67–74, 1996.

Obernosterer, I. and Herndl, G. J.: Phytoplankton extracellular release and bacterial growth: dependence on inorganic N:P ratio, Marine Ecology Progress Series, 116, 247–257, 1995.

Paasche, E.: A review of the coccolithophorid *Emiliania huxleyi* (prymnesiophyceae), with particular reference to growth, coccolith formation, and calcification-photosynthesis interactions, Phycologia, 40, 503–529, 2002.

Passow, U. and Alldredge, A. L.: A dye-binding assay for the spectrophotometric measurement of transparent exopolymer particles (TEP), Limnol. Oceanogr., 40, 1326–1335, 1995.

Passow, U.: Formation of transparent exopolymer particles, TEP, from dissolved precursor material, Marine Ecology-Progress Series, 192, 1–11, 2000.

Passow, U.: Production of transparent exopolymer particles (TEP) by phyto- and bacterioplankton, Marine Ecology-Progress Series, 236, 1–12, 2002a.

Passow, U.: Transparent exopolymer particles (TEP) in aquatic environments, Prog. Oceanogr., 55, 287–333, 2002b.

Passow, U.: The abiotic formation of TEP under different ocean acidification scenarios, Marine Chem., 128–129, 72–80, 2012.

Penna, A., Berluti, S., Penna, N., and Magnani, M.: Influence of nutrient ratios on the in vitro extracellular polysaccharide production by marine diatoms from the Adriatic Sea, J. Plankton Res., 21, 1681–1690, 1999.

Piontek, J., Händel, N., Langer, G., Wohlers, J., Riebesell, U., and Engel, A.: Effects of rising temperature on the formation and microbial degradation of marine diatom aggregates, Aquatic Microbial Ecology, 54, 305–318, 2009.

Piontek, J., Lunau, M., Händel, N., Borchard, C., Wurst, M., and Engel, A.: Acidification increases microbial polysaccharide degradation in the ocean, Biogeosciences, 7, 1615–1624, doi:10.5194/bg-7-1615-2010, 2010.

Puddu, A., Zoppini, A., Fazi, S., Rosati, M., Amalfitano, S., and Magaletti, E.: Bacterial uptake of DOM released from P-limited phytoplankton., FEMS Microbiol Ecology, 46, 257–268, 2003.

Raven, J., Caldeira, K., Elderfield, H., Hoegh-Guldberg, O., Liss, P., Riebesell, U., Shepherd, J., Turley, C., and Watson, A.: Ocean acidification due to increasing atmospheric carbon dioxide, The Royal Society, London, UK, 2005.

Riebesell, U., Zondervan, I., Rost, B., Tortell, P. D., Zeebe, R. E., and Morel, F. M. M.: Reduced calcification of marine plankton in response to increased atmospheric CO_2, Nature, 407, 364–367, 2000.

Riebesell, U., Schulz, K. G., Bellerby, R. G. J., Botros, M., Fritsche, P., Meyerhofer, M., Neill, C., Nondal, G., Oschlies, A., Wohlers, J., and Zollner, E.: Enhanced biological carbon consumption in a high CO_2 ocean, Nature, 450, 545–549, 2007.

Riegman, R., Stolte, W., Noordeloos, A. A. M., and Slezak, D.: Nutrient uptake and alkaline phosphatase (EC 3:1:3:1) activity of *Emiliania huxleyi* (Prymnesiophyceae) during growth under N and P limitation in continuous cultures, J. Phycology, 36, 87–96, 2000.

Sarmiento, J. L., Slater, R., Barber, R., Bopp, L., Doney, S. C., Hirst, A. C., Kleypas, J., Matear, R., Mikolajewicz, U., Monfray, P., Soldatov, V., Spall, S. A., and Stouffer, R.: Response of ocean ecosystems to climate warming, Global Biogeochemical Cycles, 18, GB3003, doi:10.1029/2003GB002134, 2004.

Schartau, M., Engel, A., Schröter, J., Thoms, S., Völker, C., and Wolf-Gladrow, D.: Modelling carbon overconsumption and the formation of extracellular particulate organic carbon, Biogeosciences, 4, 433–454, doi:10.5194/bg-4-433-2007, 2007.

Schneider, B., Engel, A., and Schlitzer, R.: Effects of depth- and CO_2-dependent C:N ratios of particulate organic matter (POM) on the marine carbon cycle, Global Biogeoche. Cycles, 18, GB2015, doi:10.1029/2003GB002184, 2004.

Sciandra, A., Harlay, J., Lefèvre, D., Lemée, R., Rimmelin, P., Denis, M., and Gattuso, J.-P.: Response of the coccolithophorid *Emiliania huxleyi* to elevated pCO_2 under nitrate limitation, Marine Ecology Progress Series, 261, 111–122, 2003.

Skoog, A. and Benner, R.: Aldoses in various size fractions of marine organic matter: Implications for carbon cycling, Limnol. Oceanogr., 42, 1803–1813, 1997.

Skoog, A., Alldredge, A., Passow, U., Dunne, J., and Murray, J.: Neutral aldoses as source indicators for marine snow, Marine Chemistry, 108, 195–206, 2008.

Smith, R. E. H. and Platt, T.: Carbon exchange and ^{14}C tracer methods in a nitrogen-limited diatom, *Thalassiosira pseudonana*, Marine Ecology Progress Series, 16, 75–87, 1984.

Solomon, S., Qin, D., Manning, M., Chen, Z., Marquis, M., Averyt, K. B., Tignor, M., and Miller, H. L.: Climate Change 2007: The Physical Science Basis. Contribution of Working Group I to the Fourth Assessment Report of the Intergovernmental Panel on Climate Change, Cambridge University Press, Cambridge, United Kingdom and New York, USA, 2007.

Staats, N., Stal, L. J., and Mura, L. R.: Exopolysaccharide production by the epipelic diatom *Cylindrotheca closterium*: effects of nutrient conditions, J. Experimental Marine Biology and Ecology, 249, 13–27, 2000.

Steemann Nielsen, E.: The Use of Radioactive Carbon (^{14}C) for Measuring Primary Production in the Sea, J. Cons. Perm. Int. Explor. Mer., 18, 117–140, 1952.

Teira, E., Pazó, M. J., Serret, P., and Fernández, E.: Dissolved organic carbon production by microbial populations in the Atlantic Ocean, Limnol. Oceanogr., 46, 1370–1377, 2001.

Toggweiler, J. R.: Carbon overconsumption, Nature, 363, 210–211, 1993.

Underwood, G. J. C., Boulcott, M., Raines, C. A., and Waldron, K.: Environmental effects on exopolymer production by marine benthic diatoms: Dynamics, changes in composition and pathways of production, J. Phycology, 40, 293–304, 2004.

Van der Wal, P., Kempers, R. S., and Veldhuis, M. J. W.: Production and downward flux of organic matter and calcite in a North Sea bloom of the coccolithophore *Emiliania huxleyi*, Marine ecology progress series, 126, 247–265, 1995.

Veldhuis, M. J. W., Stoll, M., Bakker, D., Brummer, G. J., Kraak, M., Kop, A., Vanweerlee, E., Vankoutrik, A., and Heimdal, B. R.: Calcifying phytoplankton in bjornafjorden, norway – the prebloom situation, Sarsia, 79, 389–399, 1994.

Verdugo, P., Alldredge, A. L., Azam, F., Kirchman, D. L., Passow, U., and Santschi, P. H.: The oceanic gel phase: a bridge in the DOM-POM continuum, Marine Chemistry, 92, 67–85, 2004.

Verdugo, P., Orellana, M. V., Chin, W. C., Petersen, T. W., van Eng, G., Benner, R., and Hedges, J. I.: Marine bio-polymer self-assembly: Implications for carbon cycling in the ocean, Faraday. Discussions, 139, 393–398, 2008.

Verity, P. G., Smayda, T. J., and Sakshaug, E.: Photosynthesis, excretion and growth rates of *Phaeocystis* colonies and solytary cells, Polar Research, 10, 117–128, 1991.

Wangersky, P. J.: The Distribution of Particulate Organic Carbon in the Oceans: Ecological Implications, Internationale Revue der gesamten Hydrobiologie und Hydrographie, 63, 567–574, 1978.

Wells, M. L.: Marine colloids: A neglected dimension, Nature, 391, 530–531, 1998.

Westbroek, P., de Jong , E. W., Dam, W., and Bosch, L.: Soluble intracrystalline polysaccharides from coccoliths of *Coccolithus huxleyi* (Lohmann) Kamptner, Calcified Tissue Research, 12, 227–238, 1973.

Wetz, M. S. and Wheeler, P. A.: Production and partitioning of organic matter during simulated phytoplankton blooms, Limnol. Oceanogr., 48, 1808–1817, 2003.

Wetz, M. S. and Wheeler, P. A.: Release of organic matter by coastal diatoms, Limnol. Oceanogr., 52, 798–807, 2007.

Williams, P. J. l. B.: The importance of losses during microbial growth: commentary on the physiology, measurement and ecology on the release of dissolved organic matter, in: Microbial Growth: Inputs and Losses, Practical Approaches, edited by: Maestrini, S. Y. and Rassoulzadegan, F., Marine Microbial Food Webs, 4, 175–206, 1990.

Wohlers, J., Engel, A., Zöllner, E., Breithaupt, P., Jürgens, K., Hoppe, H. G., Sommer, U., and Riebesell, U.: Changes in biogenic carbon flow in response to sea surface warming, Proc. Natl. Acad. Sci. USA, 106, 7067–7072, 2009.

Wood, M. A. and van Valen, L. M.: Paradox lost? On the release of energy-rich compounds by phytoplankton, Marine Microbial Food Webs, 4, 103–116, 1990.

Yamada, N. and Suzumura, M.: Effects of Seawater Acidification on Hydrolytic Enzyme Activities, J. Oceanogr., 66, 233–241, 2010.

Zlotnik, I. and Dubinsky, Z.: The effect of light and temperature on DOC excretion by phytoplankton, Limnol. Oceanogr., 34, 831–839, 1989.

Zondervan, I., Rost, B., and Riebesell, U.: Effect of CO_2 concentration on the PIC/POC ratio in the coccolithophore *Emiliania huxleyi* grown under light-limiting conditions and different daylengths, J. Experimental Marine Biology and Ecology, 272, 55–70, 2002.